Dust Evolution in Protoplanetary Disks

Leonardo Testi[1,2,3], Tilman Birnstiel[4], Luca Ricci[5], Sean Andrews[4], Jürgen Blum[6], John Carpenter[5], Carsten Dominik[7], Andrea Isella[5], Antonella Natta[2,8], Jonathan P. Williams[9], David J. Wilner[4]

[1]European Southern Observatory, Germany
[2]INAF–Osservatorio Astrofisico di Arcetri, Italy
[3]Excellence Cluster Universe, Boltzmannstr. 2, D-85748 Garching, Germany
[4]Harvard-Smithsonian Center for Astrophysics, USA
[5]California Institute of Technology, USA
[6]Institut für Geophysik und extraterrestrische Physik, TU Braunschweig, Germany
[7]University of Amsterdam, The Netherlands
[8]Dublin Institute for Advanced Studies, Ireland & INAF–Osservatorio Astrofisico di Arcetri, Italy
[9]Institute for Astronomy, University of Hawaii, USA

In the core accretion scenario for the formation of planetary rocky cores, the first step toward planet formation is the growth of dust grains into larger and larger aggregates and eventually planetesimals. Although dust grains are thought to grow from the submicron sizes typical of interstellar dust to micron size particles in the dense regions of molecular clouds and cores, the growth from micron size particles to pebbles and kilometre size bodies must occur in the high densities reached in the mid-plane of protoplanetary disks. This critical step in the formation of planetary systems is the last stage of solids evolution that can be observed directly in young extrasolar systems before the appearance of large planetary-size bodies.

Tracing the properties of dust in the disk mid-plane, where the bulk of the material for planet formation resides, requires sensitive observations at long wavelengths (sub-mm through cm waves). At these wavelengths, the observed emission can be related to the dust opacity, which in turns depend on to the grain size distribution. In recent years the upgrade of the existing (sub-)mm arrays, the start of ALMA Early Science operations and the upgrade of the VLA have significantly improved the observational constraints on models of dust evolution in protoplanetary disks. Laboratory experiments and numerical simulations led to a substantial improvement in the understanding of the physical processes of grain-grain collisions, which are the foundation for the models of dust evolution in disks.

In this chapter we review the constraints on the physics of grain-grain collisions as they have emerged from laboratory experiments and numerical computations. We then review the current theoretical understanding of the global processes governing the evolution of solids in protoplanetary disks, including dust settling, growth, and radial transport. The predicted observational signatures of these processes are summarized.

We discuss the recent developments in the study of grain growth in molecular cloud cores and in collapsing envelopes of protostars as these likely provide the initial conditions for the dust in protoplanetary disks. We then discuss the current observational evidence for the growth of grains in young protoplanetary disks from millimeter surveys, as well as the very recent evidence of radial variations of the dust properties in disks. We also include a brief discussion of the constraints on the small end of the grain size distribution and on dust settling as derived from optical, near-, and mid-IR observations. The observations are discussed in the context of global dust evolution models, in particular we focus on the emerging evidence for a very efficient early growth of grains in disks and the radial distribution of maximum grain sizes as the result of growth barriers in disks. We will also highlight the limits of the current models of dust evolution in disks including the need to slow the radial drift of grains to overcome the migration/fragmentation barrier.

1. INTRODUCTION

In this chapter we will discuss the evolution of dust in protoplanetary disks, focusing on the processes of grain growth and the observational consequences of this process. In the standard scenario for planet formation, this is the phase in which the solids grow from micron-size particles, which are present in the molecular cloud cores out of which stars and protoplanetary disks are formed, to centimeter size

and beyond on the path to become planetesimals. This is the last stage of solid growth that is directly observable before the formation of large, planetary-size bodies that can be individually observed. As this phase of growth is directly observable, it has the potential of setting strong constraints on the initial stages of the planet formation process. In this review, we focus on the growth of particles on the disk mid-plane, as this is where most of the solid mass of the disk is concentrated and where planets are expected to form. Grain growth in the disk inner regions and atmosphere can be effectively investigated in the infrared and have been extensively reviewed in *Natta et al.* (2007), although at the time of that review the observational evidence and theoretical understanding of the global dust evolution processes in the disk were limited.

This phase of growth up to centimeter size particles in protoplanetary disks can also be connected to the study of the most pristine solids in our own Solar System. We can directly follow grain growth in the Solar nebula through the study of primitive rocky meteorites known as chondrites. Chondrites are composed mainly of millimeter-sized, spherical chondrules with an admixture of smaller, irregularly-shaped calcium aluminum inclusions (CAI) embedded in a fine-grained matrix (e.g. *Scott and Krot*, 2005). Some chondrules may be the splash from colliding planetesimals but most have properties that are consistent with being flash-heated agglomerates of the micron-sized silicate dust grains in the matrix. CAIs are the first solids to condense from a hot, low pressure gas of solar composition. Their ages provide the zero point for cosmochemical timescales and the astronomical age of the Sun, 4.567 Gyr. Relative ages can be tracked by the decay of short-lived radionucleides and allow the formation timescales of dust agglomerates and planetesimals to be placed in context with astronomical observations (*Dauphas and Chaussidon*, 2011). Recent measurements of absolute ages of the chondrules found that these were formed over a period that span from CAI formation to a few Myr beyond (*Connelly et al.*, 2012). As chondrule dating refers to the time when the dust agglomerate was melted, this new result tells us either that dust grains rapidly grew up to millimeter sizes in the early solar nebula and were melted progressively over time while agglomeration into larger bodies continued over the lifetime of the protoplanetary disk; or that the growth of these millimeter and centimeter size agglomerates from smaller particles continued over a period of several million years. In any case, the process of assembling CAIs and chondrules into larger bodies had to occur throughout the disk lifetime (see also the chapter by *Johansen et al.*).

In this review we will thus concentrate on the most recent developments of the theoretical models for grain evolution in disks and the constraints on the grain-grain collisions from laboratory experiments as well as on the new wealth of data at (sub-)millimeter and centimeter wavelengths that is becoming available. The goal will be to give an overview of the current astronomical constraints on the process and timescale of grain growth in disks.

The processes and observations that we discuss in this chapter are expected to occur in protoplanetary disks and both the theoretical models and the interpretation of the observations rely on assumptions on the disk structure and its evolution. The structure and evolution of protoplanetary disks during the pre-main sequence phase of stellar evolution has been discussed extensively in recent reviews and books (e.g. *Dullemond et al.*, 2007; *Hartmann*, 2009; *Armitage*, 2010; *Williams and Cieza*, 2011). Throughout this chapter, our discussion will assume a flared, irradiated disk structure in hydrostatic equilibrium with a constant gas to dust ratio of 100 by mass, unless explicitly stated otherwise. While the detailed disk structure and its evolution under the effects of viscous accretion, chemical evolution, photoevaporation and planet-disk interaction are actively investigated in detail (see e.g. the chapters by *Alexander et al.*, *Audard et al.*, *Dutrey et al.*, and *Turner et al.*), this assumed disk structure is an adequate representation of the early phases of disk evolution and a good reference for the processes of dust evolution.

Figure 1 shows a sketch of a protoplanetary disk where we illustrate pictorially the physical processes involved in grain growth on the left side. On the right side we illustrate the regions probed by the various observational techniques and the angular resolutions offered by the forthcoming generation of facilities and instruments in the infrared and sub-millimetre regions.

In § 2, we introduce the main concepts at the basis of the transport, dynamics and evolution of solid particles in disks. First we introduce the interactions between the solids and gas and the complex dynamics of solids in disks, then we describe the basic processes of the growth of solids towards larger aggregates. In § 3 we discuss the constraint on the outcomes of grain-grain collisions from laboratory experiments and numerical computations. These provide the basic constraints to the global evolution models of solids in disks, which we describe in § 4. In § 5 we discuss the effects of growth on the dust opacities and the observational consequences. The possible recent evidence for grain evolution at and before the disk formation epoch is discussed in § 6. The observational constraints for grain growth at infrared wavelengths are described in § 7. We discuss grain properties in the disk mid-plane from (sub-)millimeter observations in § 8, beginning with the methodology in § 8.1, then the results of low resolution, multi-wavelength continuum surveys in § 8.2, ending with the most recent resolved studies in § 8.3.

2. DUST TRANSPORT AND GROWTH PROCESSES IN DISKS

2.1. Dust transport processes in disks

2.1.1. Drag forces

Dust particles embedded in a gaseous protoplanetary disks are not orbiting freely, but feel a friction when moving

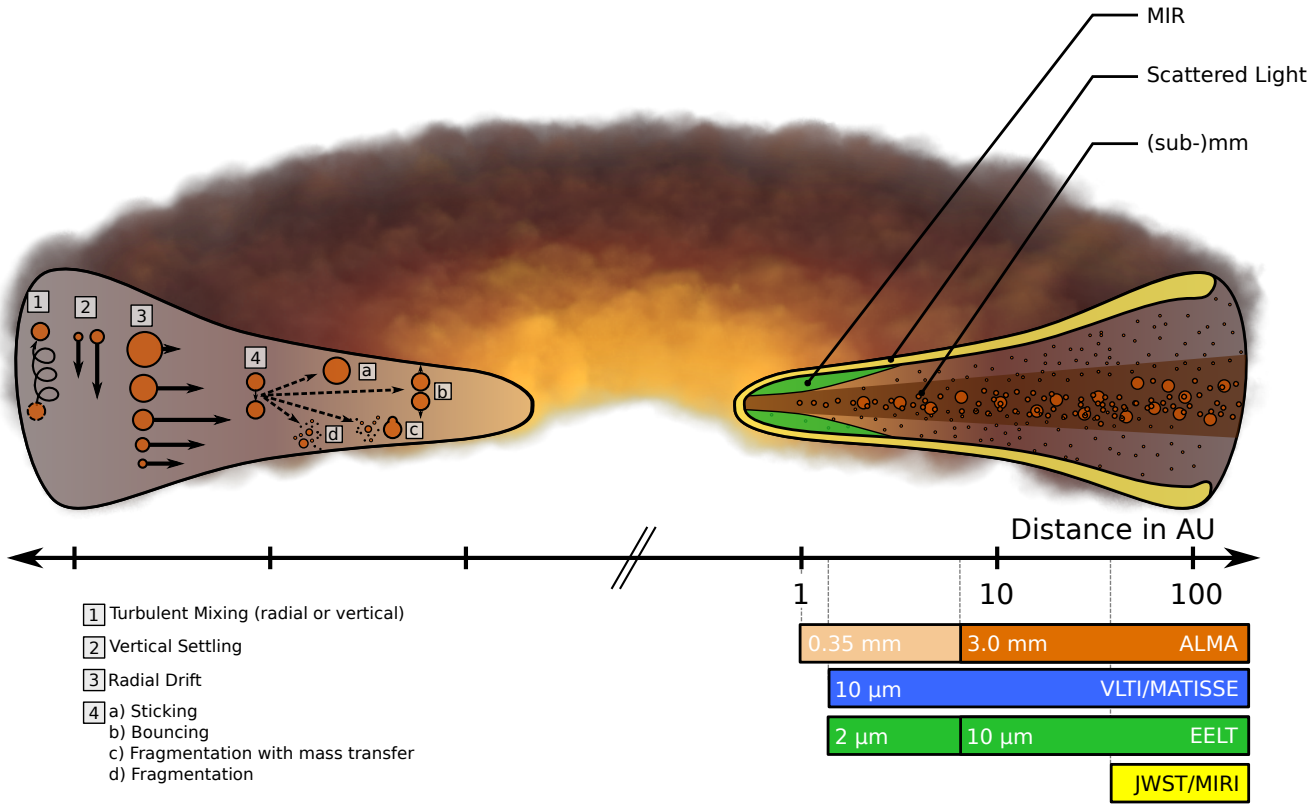

Fig. 1.— Illustration of the structure, grain evolution processes and observational constraints for protoplanetary disks. On the left side we show the main grain transport and collision mechanism properties. The different lengths of the arrows illustrate the different velocities of the different grains. On the right hand side, we show the areas of the disk that can be probed by the various techniques. The axis shows the logarithmic radial distance from the central star. The horizontal bars show the highest angular resolutions (left edge of the bars) that can be achieved with a set of upcoming facilities and instruments for at the typical distance of the nearest star forming regions.

with respect to the gas. The force exerted on them depends not only on the relative motion between gas and dust, but also on the particle size: small particles that are observable at up to cm wavelength can quite safely be assumed to be smaller than the mean free path of the gas molecules and are thus in the Epstein regime. If the particles are larger than about the mean free path of the gas molecules, a flow structure develops around the dust particle and the drag force is said to be in the Stokes drag regime (*Whipple*, 1972; *Weidenschilling*, 1977). Large particles in the inner few AU of the disk could be in this regime, and the transition into the Stokes drag regime might be important for trapping of dust particles and the formation of planetesimals (e.g. *Birnstiel et al.*, 2010a; *Laibe et al.*, 2012; *Okuzumi et al.*, 2012). An often used quantity is the stopping time, or friction time, which is the characteristic time scale for the acceleration or deceleration of the dust particles $\tau_{\rm s} = m\,v/F$, where m and v are the particle mass and velocity, and F is the drag force. Even more useful is the concept of the Stokes number, which in this context is defined as

$$\mathrm{St} = \Omega_{\rm K}\,\tau_{\rm s}, \qquad (1)$$

a dimensionless number, which relates the stopping time to the orbital period $\Omega_{\rm K}$. The concept of the Stokes number is useful because particles of different shapes, sizes, or composition, or in a different environment have identical aerodynamical behavior if they have the same Stokes number.

2.1.2. *Radial drift*

The simple concept of drag force leads to important implications, the first of which, *radial drift*, was realized by *Whipple* (1972), *Adachi et al.* (1976), and by *Weidenschilling* (1977): an orbiting parcel of gas is in a force balance between gravitational, centrifugal, and pressure forces. The pressure gradient is generally pointing outward because densities and temperatures are higher in the inner disk. This additional pressure support results is a slightly sub-Keplerian orbital velocity for the gas. In contrast, a freely orbiting dust particle feels only centrifugal forces and gravity, and should therefore be in a Keplerian orbit. This slight velocity difference between gas and a free floating dust particle thus causes an efficient deceleration of the dust particle, once embedded in the gaseous disk. Consequently, the particle looses angular momentum and spirals towards

smaller radii. This inward drift velocity is only a small fraction of the total orbital velocity (a few per mille), but, for St$\sim$1 particles, it still leads to an inward drift speed of the order of 50 m s^{-1}. It also means that particles of different sizes acquire very different radial velocities and also that at any given radius, dust of the right size may be quickly moving towards the central star.

Nakagawa et al. (1986) investigated the equations of motion for arbitrary gas to dust ratios. For a value of 100 by mass, gas is dynamically dominating and the classical results of *Weidenschilling* (1977) are recovered, however for a decreasing ratio, the drag that the dust exerts on the gas becomes more important, and eventually may be reversed: dust would not drift inward and gas would be pushed outward instead. Much lower gas-to-dust ratios, approaching unity, however, also lead to other effects such as the streaming instability (*Youdin and Goodman*, 2005) or self-induced stirring (for details, see the chapter by *Johansen et al.*).

The radial drift process does not necessarily mean that all particles are falling into the star, as dust may pile up at some specific locations in the innermost regions of the disk where the gas to dust ratio will become very low (this process has actually been suggested as an explanation for the abundance of rocky exoplanets close to the host star *Chatterjee and Tan*, 2014), however a significant fraction of large grains need to be kept in the outer disk for long timescales, otherwise it would result in a stark contrast to the observed population of mm-sized grains in the outer disk (see Sect. 8).

In the next paragraph we will discuss some processes that may oppose and slow down the radial drift.

2.1.3. Dust Trapping

Many works have addressed details of radial drift (*Whipple*, 1972; *Weidenschilling*, 1977; *Youdin and Shu*, 2002; *Takeuchi and Lin*, 2002; *Brauer et al.*, 2007, e.g.), however the main conclusions remain: unless the gas to dust ratio is very low, or disks are much more massive than seems reasonable, *observable* particles should drift to the inner regions within only a small fraction of the life times of protoplanetary disks. *Observable* here means detectable with current (sub-)millimeter observatories, i.e., mainly dust in the outer regions (beyond $\sim$20 AU) of the disk at current resolutions. The only other way to stop particles from spiraling inward is to locally reverse the pressure gradient, as can be seen from the drift velocity (*Nakagawa et al.*, 1986)

$$u_{\rm drift} = \frac{1}{{\rm St} + {\rm St}^{-1}\,(1+\epsilon)^2}\,\frac{c_{\rm s}^2}{V_{\rm K}}\,\frac{\partial \ln P}{\partial \ln r}, \qquad (2)$$

where P is the gas pressure, $c_{\rm s} = \sqrt{k_{\rm B}\,T/\mu\,m_{\rm p}}$ the isothermal sound speed, $V_{\rm K}$ the Keplerian velocity, and ϵ the dust-to-gas ratio. If the pressure gradient is zero or positive, there is no radial drift or particles drift outward.

This basic mechanism of dust drifting to regions of higher pressure has been explored in different settings: *Barge and Sommeria* (1995) showed that anticyclonic vortices represent a high-pressure region, which can accumulate dust particles (see also *Klahr and Henning*, 1997; *Fromang and Nelson*, 2005). The dust drift mechanism also works efficiently in the azimuthal direction if there exist regions of azimuthal over-pressure (e.g. *Birnstiel et al.*, 2013), however it should be stressed, that the mechanism relies on relative motion between gas and dust: as an example of this exception, an over-density caused by an eccentric disk, does not trap dust particles, as shown by *Hsieh and Gu* (2012) and *Ataiee et al.* (2013). For an eccentric disk, the over-density, and thus the pressure maximum, arises due to the non-constant azimuthal velocity along the elliptic orbits, but the same holds for the dust, i.e., the velocity difference between dust and the partially pressure supported gas remain, and consequently, the radial drift mechanism is still active, but the dust is not concentrated azimuthally with respect to the gas.

2.1.4. Radial mixing and meridional flows

The drift motion towards higher pressure is not the only mode of transport of dust, there are two additional ones: mixing and advection. These are interesting as they may oppose radial drift under certain circumstances and may provide an explanation for mixing processed dust outward in the disk. Outward mixing processes, including winds (e.g. *Shu et al.*, 1994, 2001), have been invoked to explain the presence of crystalline solids in disks (*Keller and Gail*, 2004; *Ciesla*, 2009) and comets in our own Solar System (*Bockelée-Morvan et al.*, 2002). Evidence for dust processing in the inner regions of disks and subsequent radial transport has been recently observed directly by Spitzer (*Ábrahám et al.*, 2009; *Juhász et al.*, 2012). In this review we will not discuss these topics that have been extensively covered elsewhere (e.g. *Natta et al.*, 2007; *Dullemond and Monnier*, 2010; *Williams and Cieza*, 2011), below we just provide a brief account of the radial transport processes.

Advection is a result of the viscous evolution of the gas which essentially drags dust particles along with the radial gas velocity, as long as they are efficiently coupled to the gas. This drag velocity was derived, for example in *Takeuchi and Lin* (2002) as

$$u_{\rm r,drag} = \frac{u_{\rm r,gas}}{1+{\rm St}^2}, \qquad (3)$$

which states that only small particles (St<1) are effectively coupled with the gas. It was first shown by *Urpin* (1984), that the gas velocity of a region with net inward motion can be positive at the mid-plane. This flow pattern, called *meridional flow*, allows for outward transport of dust grains. This process is typically much weaker than radial drift and thus unable to explain millimeter sized particles in the outer disk. In addition, large-scale circulation pattern of meridional flows, while present in viscous disk simulations (*Kley and Lin*, 1992; *Rozyczka et al.*, 1994), are not reproduced in MRI turbulent simulations (*Fromang et al.*, 2011).

In addition to this systematic motion, the gas is also thought to be turbulent (see also the chapters by *Dutrey et al.* and by *Turner et al.*), and the dust is therefore mixed by this turbulent stirring as well. The fact that the dust is not necessarily perfectly coupled to the gas motion leads to some complications (see, *Youdin and Lithwick*, 2007). The ratio between gas viscosity $\nu_{\rm gas}$ and gas diffusivity $D_{\rm gas}$ is called the Schmidt number. It is usually assumed that the gas diffusivity equals the gas viscosity, in which case the Schmidt number for the dust is defined as

$$\mathrm{Sc} = \frac{D_{\rm gas}}{D_{\rm dust}}. \quad (4)$$

Youdin and Lithwick (2007) included effects of orbital dynamics, which were neglected in previous studies of *Cuzzi et al.* (1993) and *Schräpler and Henning* (2004), and showed that the Schmidt number can be approximated by $\mathrm{Sc} \simeq 1 + \mathrm{St}^2$. It is currently believed that none of these radial transport mechanisms can overcome the radial drift induced by the pressure gradient because the vertically-integrated net transport velocity is dominated by the much stronger radial drift velocity (e.g. *Jacquet*, 2013).

2.1.5. Vertical mixing & settling

A dust particle elevated above the gas mid-plane, orbiting at the local Keplerian velocity, would vertically oscillate due to its orbital motion, if it were not for the gas drag force, which damps motion relative to the gas flow. Following the concepts discussed in the previous sections, particles with Stokes number smaller than unity are thus damped effectively within one orbit. Larger particles will experience damped vertical oscillations. The terminal velocity of small particles can be calculated by equating the vertical component of the gravitational acceleration and the deceleration by drag forces. The resulting settling velocity for $\mathrm{St} < 1$, $v_{\rm sett} = \mathrm{St}\,\Omega_{\rm K}\,z$, increases with particle size and height above the mid-plane.

Vertical settling was already the focus of the earliest models of planetesimal formation, such as *Safronov* (1969), *Goldreich and Ward* (1973), *Weidenschilling* (1980), and *Nakagawa et al.* (1986), and has remained an active topic of debate (e.g. *Cuzzi et al.*, 1993; *Johansen and Klahr*, 2005; *Carballido et al.*, 2006; *Bai and Stone*, 2010). The main question, however, is usually not the effectiveness of settling motion itself, but the effectiveness of the opposing mechanism: turbulent mixing. *Dubrulle et al.* (1995) calculated the vertical structure of the dust disk, by solving for an equilibrium between settling and mixing effects. The resulting scale height of the dust concentration in an isothermal disk with scale height $H_{\rm p} = c_{\rm s}/\Omega_{\rm K}$ then becomes $H_{\rm dust} = H_{\rm p}/\sqrt{1 + \mathrm{St}/\alpha_{\rm t}}$, where we used the canonical turbulence prescription with parameter $\alpha_{\rm t}$ (*Shakura and Sunyaev*, 1973). Detailed MHD models of MRI turbulent disks of *Fromang and Nelson* (2009) show, that the simple result from *Dubrulle et al.* (1995) is a good approximation only near the mid-plane. Above roughly one scale height, the vertical variations in the strength of the turbulence and other quantities cause strong variations from the result of *Dubrulle et al.* (1995).

The effects that dust settling has on the observational appearance of disks have been derived for example by *Chiang et al.* (2001), *D'Alessio et al.* (2001), or *Dullemond and Dominik* (2004). While the settling process could lead to the rapid growth of particles and the formation of a thin mid-plane layer of large pebbles, it is expected that small dust is replenished in the disk upper layers, e.g. by small fragments from shattering collisions between dust grains (e.g. *Dullemond and Dominik*, 2005; *Birnstiel et al.*, 2009; *Zsom et al.*, 2011) or by continuous infall (e.g. *Mizuno et al.*, 1988; *Dominik and Dullemond*, 2008).

2.2. Grain growth processes

The transport mechanisms discussed in the previous sections all lead to large differential vertical and radial motion of dust particles. These in turn imply frequent grain-grain collisions, potentially leading to growth. The two main ingredients for a model of dust growth are the collision frequency and the collision outcome. The growth process is modeled as the result of primordial dust particles, referred to as *monomers*, that can stick together to form larger *aggregates*. The latter depends on many different parameters, such as the composition (e.g. fraction of icy, silicate, or carbonaceous particles), the monomer size distribution, the structure (i.e., compact, porous, fractal grains, layers, etc.), the impact parameter and impact velocity. We will first discuss here the expected ranges of impact velocities and then, in § 3, some of the recent laboratory constraints on the collision outcomes.

The final ingredient, the collision frequency, depends on the one hand on the cross section of the particles and their number density, which are results of the modeling itself, and on the other hand on the relative velocity of grains. We will describe these in the context of the global dust evolution models in § 4.

2.2.1. Relative velocities

The relative velocities between particles in disks under the combined effects of settling and radial drift can directly be derived from the terminal dust velocities of *Nakagawa et al.* (1986) for two different-sized particles (e.g. *Weidenschilling and Cuzzi*, 1993; *Brauer et al.*, 2008a) and many others. As an example, the upper panel of Fig. 2 shows the expected relative velocities between grains of different sizes as computed for 1 AU by *Weidenschilling and Cuzzi* (1993). Both radial drift and vertical settling velocities peak at a Stokes number of unity. Relative motions increase with the size difference of the particles because particles with the same Stokes number have the same systematic velocities. The maximum relative velocity via radial drift is

$$\Delta v_{\rm drift} = \frac{c_{\rm s}^2}{V_{\rm K}} \frac{\partial \ln P}{\partial \ln r}. \quad (5)$$

Relative azimuthal velocities are small for particles of Stokes number less than unity, approach a constant, high value for $\mathrm{St} > 1$, and also increase with the Stokes number difference.

In addition to these systematic motions, random motions also induce relative velocities, even between particles of the same Stokes number. Brownian motion of the particles is negligible for large particles, but it is the dominating source of relative motion for small particles, roughly sub-μm sizes.

Much more complicated than the relative motion discussed above and a topic of current research is turbulent motion. The most frequently used formalism of this problem was introduced by *Voelk et al.* (1980) and *Markiewicz et al.* (1991), and recently, closed-form expressions were derived by *Cuzzi and Hogan* (2003) and *Ormel and Cuzzi* (2007). Their results show that, similar to radial drift and vertical settling, turbulent relative velocities increase with the Stokes number difference between the colliding particles and generally increase with the Stokes number until a $\mathrm{St} = 1$. Beyond, it drops off again, but slower than for example relative velocities induced by radial drift or vertical settling.

The maximum turbulent velocity according to *Ormel and Cuzzi* (2007) is

$$\Delta v_{\mathrm{turb}} = c_{\mathrm{s}} \left(9\alpha_{\mathrm{t}}/2\right)^{1/2} \tag{6}$$

and a factor of $\sqrt{3}$ smaller for collisions between equal-sized particles. For typical parameter choices ($\partial \ln P / \partial \ln r$ = 2.75), Eqs. 5 and 6 imply that the turbulence parameter α_{t} has to be only larger than about $2(H_{\mathrm{p}}/r)^2$ to be the dominant source of relative velocity between grains. The dominant contributions to the relative velocities are also shown in the top panel of Fig. 3. For planetesimals, also the gravitational torques of the turbulent gas play a role (not shown in Fig. 3, but see chapter by *Johansen et al.*)

The works mentioned above generally treat only the r.m.s. velocity between dust grains, but the distribution of the collision velocity can also be important. Recently, some numerical works have tested the analytically derived collision velocities and started to derive distributions of collision velocities, e.g. *Carballido et al.* (2010); *Pan and Padoan* (2010); *Hubbard* (2012); *Pan and Padoan* (2013). We will come back to the treatment of grain velocities in the context of global disk models in § 4.2.

2.2.2. *Condensation*

A different physical process for growing (destroying) dust grains without grain collisions is condensation (evaporation) of material from the gas phase or the sublimation of mantles and solids. Dust growth via this mechanisms was mentioned already in early works (*Goldreich and Ward*, 1973). It is commonly discussed in the context of dust formation and evolution in the interstellar medium (e.g. *Zhukovska et al.*, 2008; *Hirashita and Kuo*, 2011), but also in the context of the "condensation sequence" (e.g. *Lodders*, 2003). The problem with growing large grains via condensation in a protoplanetary disk is twofold: firstly, there is usually not enough material in the gas phase to grow a macroscopic dust/ice mantle on every microscopic grain, secondly, accretion is a surface effect and the dust surface area is strongly dominated by the smallest grains. Condensation will therefore happen preferentially on the smallest grains, until all condensable material is consumed. Growth of large grains by condensation in protoplanetary disks can therefore only happen if there is some continuous source of condensable material, (e.g. near an evaporation zone) and if some mechanism is able to preferentially transport the condensing material onto the largest particles. Some recent work by *Ros and Johansen* (2013) simulated growth of decimeter sized particles consisting entirely of ice. However this work relies on the absence of both dust and radial drift, i.e. dust nuclei are not left over after evaporation and vapor thus recondenses on another ice particle instead. Whether large particles can be formed by condensation under realistic disk conditions remains a topic for future research.

3. CONSTRAINTS ON THE PHYSICAL PROCESSES FROM LABORATORY EXPERIMENTS

The constraints on the collision outcomes as a function of particle size, composition, shape and relative velocities are an essential input to the models of grain evolution in disks. It is not easy to explore the full parameter space for the conditions present in protoplanetary disks, here we will cover the emerging trends from laboratory experiments and numerical computations of grain-grain (or aggregate-aggregate) low-velocity collisions (for recent reviews, see also *Dominik et al.*, 2007; *Blum and Wurm*, 2008). Dust grains in protoplanetary disks are subject to relatively low-velocity mutual collisions, which can have a very wide spectrum of results ranging from the complete fragmentation of the two particles leading to a swarm of smaller fragments to the formation of a single larger particle containing the total mass of the system. The experimental techniques of investigating dust-particle and dust-aggregate collisions have considerably improved over the past decades so that reliable conclusions on the dust evolution in disks can be drawn.

The main questions that we will address are the following:

1. Why do dust particles or dust aggregates grow?
2. What are the structures of growing dust particles?
3. How fast do dust aggregates grow?
4. What is the maximum size that dust aggregates can reach?
5. Is the formation of larger aggregates by direct sticking collisions possible?

We will review the status of research on the above points one by one. In Fig. 2 we provide a schematic representation of the various processes discussed below.

3.1. Why do dust particles or dust aggregates grow?

The cause of dust growth is probably the easiest to answer. It is generally assumed that in the dense regions of protoplanetary disks not too close to the central star, electrostatic charges and magnetic materials do not play a dominant role in the interaction between grains, however, this is currently debated and several studies have investigated their effects on grain evolution in disks (*Dominik and Nübold*, 2002; *Matthews et al.*, 2012; *Okuzumi et al.*, 2011b). In the absence of these effects, dust grains in contact still possess an adhesive (van der Waals) force (*Heim et al.*, 1999; *Gundlach et al.*, 2011). If the dissipation of kinetic energy during the collision is strong enough, hysteresis effects at the contact point can lead to the sticking of the dust grains (*Chokshi et al.*, 1993; *Dominik and Tielens*, 1997). This direct hit-and-stick coagulation process has been experimentally investigated by *Poppe et al.* (2000). They found that $\sim 1\mu\mathrm{m}$ sized silica grains can stick to one another if they collide at less than $\sim 1\mathrm{m\ s^{-1}}$. Smaller grains can stick at higher velocities, whereas larger grains possess a lower threshold for sticking. This threshold velocity, below which sticking is dominant, is possibly strongly affected by the grain material. Recent investigations have shown that micrometer-sized water-ice particles seem to stick up to about $30\ \mathrm{m\,s^{-1}}$ collision velocity, in agreement with the much higher surface energy of water ice (*Gundlach et al.*, 2011). Such high sticking thresholds have been used before in numerical simulations of ice-aggregate growth (see, e.g. *Wada et al.*, 2009, and the chapter by *Johansen et al.*). That larger particles have a lower sticking threshold is in principle still true for dust aggregates, although the details of the hit-and-stick process for soft-matter (or granular) particles are somewhat different. Based on laboratory experiments on collisions among (sub-)mm-sized high-porosity dust aggregates (consisting of $\sim 1\mu\mathrm{m}$ sized silica grains), *Kothe et al.* (2013) derived a mass-dependent threshold velocity of the form $v \propto m^{-3/4}$. However, the threshold velocity for sticking of dust aggregates depends on many parameters, e.g. on grain size and material (sub-μm vs μm, silicates vs ice), aggregate morphology (fractal, fluffy, compact, hierarchical), or mass ratio (through reduced mass).

3.2. What are the structures of growing dust particles?

As long as the collision velocity is well below the threshold for sticking (see above), a mutual collision is in the so-called hit-and-stick regime, in which the projectile particle sticks to the target aggregate at the point of first contact. Numerical simulations as well as experiments have shown that in this regime, the dust aggregates grow to extremely fluffy structures, which have a fractal dimension D of well below 2. This is particularly true as long as Brownian motion dominates the collisions, which lead to fractal clusters with $D \approx 1.5$ (*Blum et al.*, 2000; *Krause and Blum*, 2004; *Paszun and Dominik*, 2006). This is typically the case during the very first stages of growth, when the dust aggregates are not much larger than tens of microns. With increasing dust-aggregate mass, the hit-and-stick regime is being replaced by the compaction stage (*Blum and Wurm*, 2000; *Dominik and Tielens*, 1997) so that the fractal dimension increases (whether to values $D = 3$ or slightly below is still under debate) and dust aggregates are better described by their density or porosity. Typical volume filling factors of 0.05-0.50 are being expected for most of the mass range (*Zsom et al.*, 2010), although *Wada et al.* (2008) derived in their numerical simulations growing aggregates with D=2.5 (and correspondingly extremely small volume filling factors) when 0.1 μm-sized ice/dust monomers were considered. For monomer-size distributions according to the one derived by Mathis et al. (1977, MRN-type distribution) for interstellar dust particles, the bulk of the mass of an aggregate is dominated by the largest monomers, whereas the number of particles and, thus, the contacts between monomer grains, are determined by the smallest particles. Ormel et al. (2009) show that such an aggregate has the same strength as an aggregates of single-size monomers of 0.056 μm. These results may also hold for aggregates consisting of ice and silicate particles. Here, the weaker-bound silicate grains might determine the strength and growth properties of the ice-dust bodies.

3.3. How fast do dust aggregates grow?

Both experiments and numerical computations show that the first stage of growth is characterized by sticking. In this early phase their growth rate is simply given by the product of the number density of available collision partners, their mutual collision cross section, and their relative velocity. Under the assumption of non-fractal growth, the latter two are easily determined, while the first is a result of the growth process (see *Blum*, 2006, for a detailed description of dust-growth processes). The initial growth is also connected with a compaction of the aggregates as larger and larger grains collide and stick absorbing part of the kinetic energy rearranging their internal structure. This phase is followed by the so called "bouncing barrier", when compact grains will not easily grow through the hit-and-stick mechanism (*Zsom et al.*, 2010). The detailed outcome of the full process of grain growth will be discussed in the context of the global models in § 4, numerical experiments show that, due to compaction processes, the dust aggregates start very fluffy but are ultimately relatively compact. It is thus realistic to constrain the collision of particles beyond the "bouncing barrier" with the results of laboratory experiments based on compact aggregates.

3.4. What is the maximum size that dust aggregates can reach?

Although many uncertainties about the collision properties of growing protoplanetary dust aggregates exist (see,

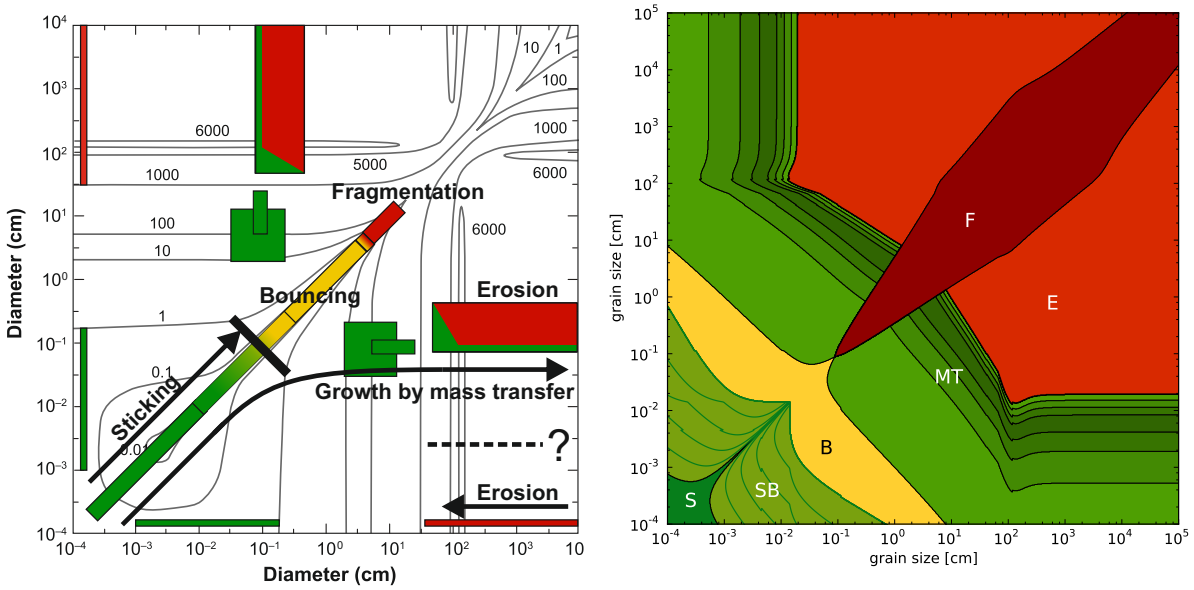

Fig. 2.— Schematic representation of the outcomes of dust collisions in protoplanetary disks. Left panel: the background plot shows the collision velocities (in units of cm/s) between two non-fractal dust agglomerates with sizes indicated on the axes in a minimum-mass solar nebula (MMSN) model at 1 AU *Weidenschilling and Cuzzi* (1993). The green, yellow, and red boxes denote the explored parameter space and results of laboratory experiments. Here, green represents sticking or mass transfer, yellow bouncing, and red fragmentation or erosion. The arrow denoted "Sticking" indicates the direct growth of mm-sized dust aggregates as found in the simulations by *Zsom et al.* (2010). Further growth is prevented by bouncing. A possible direct path to the formation of planetesimals is indicated by the arrow "Growth by mass transfer". Right panel: the collisions outcomes parameter space as used by numerical models of dust evolution in protoplanetary disks by *Windmark et al.* (2012b), as derived interpolating the results of the laboratory experiments across the entire parameter space. Note that these collisional outcomes refer only to collisions between bare silicates grains.

e.g., the discussion in *Kothe et al.*, 2013), it seems to be evident from laboratory experiments that direct sticking between dust aggregates in mutual collisions is limited (a possible mass-velocity threshold relation has been mentioned above). Thus, there is a maximum dust-aggregate size that can be formed in direct sticking collisions. The limiting factor for further growth is the bouncing and compaction of the dust aggregates, which has been observed in many laboratory experiments (see Fig. 2). However, another physical process which has been found in the laboratory is a possible loophole out of this "bouncing barrier". Above a certain velocity threshold, which is typically close to the fragmentation barrier ($\sim$ 1 m s^{-1}), collisions between small and large dust aggregates can lead to a substantial mass transfer from the smaller to the larger object (*Kothe et al.*, 2010; *Teiser et al.*, 2011; *Teiser and Wurm*, 2009a,b; *Wurm et al.*, 2005, see also Fig. 2). Recent numerical simulations indicate that the gap between the onset of bouncing and the onset of the mass-transfer process can be bridged (*Windmark et al.*, 2012b,a; *Garaud et al.*, 2013) so that growth to planetesimal sizes seems to be possible. As most of the laboratory experiments have been performed with silicates, the above statements might not be applicable to icy particles, i.e. for distances to the central star beyond the snow line. *Okuzumi et al.* (2012) studied the mass evolution of aggregates consisting of 0.1 μm ice aggregates and found that there is no bouncing barrier so that icy planetesimals with extremely high porosity (density below a few 10^{-4} g cm^{-3}) may be formed by direct collisional growth.

3.5. Is planetesimal formation by direct sticking collisions possible?

As indicated above, mass transfer from projectile to target agglomerate has been identified in the laboratory and confirmed in numerical simulations as a potential process by which in principle arbitrarily large dust aggregates, i.e. planetesimals, can be formed. This mass-transfer process in collisions at velocities at which the smaller of the dust aggregates fragments, can continually add mass to the growing larger dust aggregate as long as the absolute size and impact velocity of the (smaller) projectile aggregate is below a threshold curve derived by *Teiser and Wurm* (2009b). However, *Schräpler and Blum* (2011) showed in laboratory experiments that there is also a lower threshold mass for the mass-transfer process to be active (see Fig. 2). When growing dust aggregates are continuously bombarded by monomer dust grains of micrometer size, they can be eroded quite efficiently. Thus, the formation of planetesimals by mass transfer can only be possible if the mass distribution of dust aggregates does not favor erosion (too many

monomer dust grains) or fragmentation (too many similar-sized large dust aggregates). Much more work, both in the laboratory and with numerical simulations, is required before the question whether planetesimals can form by collisional sticking can be finally answered.

4. MODELS OF DUST EVOLUTION IN DISKS

4.1. Introduction and early works

The previous sections have laid the basis of dust evolution, such as transport processes, collision velocities, and collisional outcomes. In this section, we will now bring all of this together and review how grains in protoplanetary disks grow, how they are transported, and how growth and transport effects work with or against each other.

Some of the earliest works on dust particle growth in the context of planet formation were done by *Safronov* (1969), who considered both a toy model (growth of a single particle sweeping up other non-growing particles) as well as analytical solutions to the equation, which governs the time evolution of a particle size distribution, often called the Smoluchowski equation (*Smoluchowski*, 1916). A rather general way of writing this equation is

$$\dot{n}(x) = \iint_{x_1,x_2}^{\infty} n(x_1)n(x_2)K(x_1,x_2)L(x_1,x_2,x)\mathrm{d}x_1\mathrm{d}x_2. \tag{7}$$

Here x denotes a vector of properties such as composition, porosity, charge, or others, but to keep it simple, we can think of it just as particle mass m. Eq. 7 means that the particle number density $n(m)$ changes if particles with masses m_1 and m_2 collide at a rate of $K(m_1, m_2)$, where $L(m_1, m_2, m)$ denotes the mass distribution of the collisional outcome. For example, for perfect sticking, $L(m_1, m_2, m)$ is positive for all combinations of m_1 and $m_2 = m - m_1$, creating a particle of mass m, negative for all cases where $m = m_1$ or $m = m_2$, and 0 for all other combinations. Care has to be taken that the double integral does not count each collision twice. In principle, the collision rate K and outcome L can be a function of other properties as well, but in most applications the collision rate is simply a product of collisional cross section and relative velocity.

The early works of *Safronov* (1969), *Weidenschilling* (1980), and *Nakagawa et al.* (1981) considered dust grains settling towards the mid-plane and sweeping up other dust grains on the way. It was found that within few 10^3 orbits, cm-sized dust grains can form near the mid-plane and the gravitational instability of this dust layer was investigated. *Weidenschilling* (1984) showed that turbulence could cause high collision velocities and lead to break-up of aggregates instead of continuing growth.

Numerical modeling of the full coagulation equation was found to be very difficult, as the dynamical range already from sub-micrometer to decimeter sizes spans 18 orders of magnitude in mass and it was shown that a rather high number of mass sampling points is needed, in order to reach agreement between numerical and analytical results (e.g. *Ohtsuki et al.*, 1990; *Lee*, 2000). Many works therefore considered simplified models that use averaged values and only a single size.

In the following, we will focus on more recent works, first, local models of collisional dust evolution, followed by simplified and full global models. For more historical reviews on the subject, we refer to previous reviews of *Weidenschilling and Cuzzi* (1993), *Beckwith et al.* (2000), or *Dominik et al.* (2007).

4.2. Recent growth models and growth barriers

Due to the complications mentioned above, modeling dust growth, even only at a single point in space can be challenging, depending on which effects and parameters are taken into account. One of the most detailed methods of dust modeling is the N-body like evolution of monomers, as done by *Kempf et al.* (1999), however it is impossible to use this method for following the growth processes even only to mm sized particles, due to the sheer number of involved monomers.

Monte-Carlo methods make it computationally much more feasible to include several additional dust properties, such as porosity, and were first applied in the context of protoplanetary disks by *Ormel et al.* (2007, 2008). Similar Monte-Carlo methods as well as the experiment-based, detailed collision model of *Güttler et al.* (2010) were used in *Zsom et al.* (2010), which followed the size and porosity evolution of a swarm of particles. In agreement with previous studies, the initial growth occurs in the hit-and-stick phase which leads to the formation of highly porous particles. As particle sizes and impact velocities increase, the main collision outcome shifts to bouncing with compaction, in which two colliding particles do not stick to each other, but are only compacted due to the collision. The final outcome in these models was a deadlock where all particles are of similar sizes and the resulting impact velocities are such that only bouncing collisions occurred, i.e., further growth was found to be impossible and this situation was called the *bouncing barrier*.

Even if bouncing is not considered, and particles are assumed to transition from sticking directly to a fragmenting/eroding collision outcome, (as in the statistical Smoluchowski models of *Brauer et al.*, 2008a), a similar problem was found: as particles become larger, they tend to collide at higher impact velocities (see Sect. 2.2.1). At some point the impact velocity exceeds the threshold velocity for shattering. Equating this threshold velocity above which particles tend to experience disruptive collisions with an approximation of the size-dependent relative velocity, yields the according size threshold of (see, *Birnstiel et al.*, 2012, and Fig. 3)

$$a_{\mathrm{frag}} \simeq \frac{2}{3\pi}\frac{\Sigma_{\mathrm{gas}}}{\rho_{\mathrm{s}}\,\alpha_{\mathrm{t}}}\frac{u_{\mathrm{frag}}^2}{c_{\mathrm{s}}^2}, \tag{8}$$

where $\Sigma_{\rm gas}$ is the gas surface density, $\rho_{\rm s}$ the material density of the dust grains and $u_{\rm frag}$ the fragmentation threshold velocity derived from lab measurements. Earlier models were using energy arguments to decide whether fragmentation happens (e.g. *Weidenschilling*, 1997), or did not include the effects of erosion (e.g. *Dullemond and Dominik*, 2005). More recent models of *Windmark et al.* (2012a), which use an experiment-based collisional outcome model indicate that most of the dust mass is still expected to remain in small, observationally accessible particles ($\lesssim$1 cm) while allowing the formation of a small number of large bodies.

If fragmentation is limiting further growth of particles, a steady-state distribution is quickly established in which grains undergo numerous cycles of growth and subsequent shattering, i.e. growth and fragmentation balance each other. The resulting grain size distributions tend to be power-laws or broken power-laws, which do not necessarily follow the MRN-distribution (see, *Birnstiel et al.*, 2011). A common feature of these distributions is the fact that most of the dust mass is concentrated in the largest grains. However, the total dust surface area is typically dominated by small grains of about a few micrometers in radius. Below a few micrometers, the main source of collision velocities switches from turbulence to Brownian motion (see Fig. 3), which leads to a kink in the size distribution, such that particles much smaller than a micrometer do not contribute much to the total grain surface area (see, *Birnstiel et al.*, 2011; *Ormel and Okuzumi*, 2013).

Another recent development in dust modeling was the introduction of a method to self-consistently evolve the porosity in addition to the size distribution with the conventional Smoluchowski method, by *Okuzumi et al.* (2009). Including another particle property, such as porosity, increases the dimensionality of the problem from one dimension (mass) to two dimensions (mass and porosity), which makes conventional grid-based methods prohibitively slow. By including an additional property in the Smoluchowski equation and assuming it to be narrowly distributed, *Okuzumi et al.* (2009) derived the moment equations, which describe the time evolution of the size distribution and the time evolution of the mean porosity of each particle size. These moment equations are one-dimensional equations of the particle mass, which can be solved individually with the conventional Smoluchowski solvers. The results of this method showed good agreement with Monte-Carlo methods at significantly increased computational speeds.

This method was also used for including grain charge in *Okuzumi et al.* (2011a) to confirm a scenario of *Okuzumi* (2009), in which dust grain charging and the subsequent repelling force could halt grain growth. This was termed *charging barrier*. They found general agreement with their previous scenario. In particular, they found that considering a distribution of relative velocities (for Brownian motion and turbulence), in contrast to assuming that all grains collide with the r.m.s. velocity, does not allow growth beyond the charging barrier. If turbulent mixing is considered, however, the charging barrier could be overcome (*Okuzumi et al.*, 2011b).

The effects of velocity distributions were taken into account in *Windmark et al.* (2012a) and *Garaud et al.* (2013) to show that also the bouncing barrier can be overcome: not all particles collide with the r.m.s. velocity. Instead, also collisions at higher velocities (possibly causing fragmentation or erosion) or lower velocities (possibly causing sticking) occur. These additional outcomes open up a channel of growth as some particles might always be in the "lucky" regime of velocity space and continue to stick, while all particles can also sweep up the fragments produced by high-velocity impacts. In this sense, when a distribution of collision speeds and/or turbulent mixing is taken into account, both the charging as well as the bouncing barrier become "porous barriers". They can slow down particle growth, but they cannot prevent the formation of larger bodies.

Even if particles beyond the usual growth barriers are formed, i.e., particles with sizes of around centimeters or meters, depending on the position in the disk, it still seems unrealistic to assume that these boulders stick to each other at *any* velocity. Laboratory results of *Wurm et al.* (2005), however might give a solution to this problem: it was found that impacts of small grains onto larger targets at velocities of the order of 25-50 m $\rm s^{-1}$ still lead to net growth of the target, while some of the projectile mass is redistributed to smaller fragments (see also *Teiser and Wurm*, 2009a,b; *Kothe et al.*, 2010). This mechanism of *fragmentation with mass transfer* was shown to be a way in which larger particles, embedded in a large number of small dust grains, can continue to grow by sweeping up the small grains at high impact velocities (*Windmark et al.*, 2012b).

4.3. Simplified global models

Modeling the evolution of a full particle size distribution faces many conceptual challenges and comes at significant computational costs. These complications have led to several models of the global evolution of dust in protoplanetary disks that focus on the transport side of the evolution and use only a simplified size evolution.

Some earlier works focused only on the very early evolution or on a limited radial range (e.g. *Morfill and Voelk*, 1984; *Sterzik and Morfill*, 1994). Models of *Stepinski and Valageas* (1996, 1997), and *Hughes and Armitage* (2012) followed also the mono-disperse growth of dust particles, however they only considered pure sticking, i.e. particles could grow without limits. They showed that particles can be quickly depleted from the disk if they grow and drift. While in *Youdin and Shu* (2002), particles of a fixed size accumulate because the drift velocity becomes slower in the inner regions of the disk, in the case of *Stepinski and Valageas* (1997) and also *Kornet et al.* (2001), particles grow as they drift inward, which counteracts the decrease

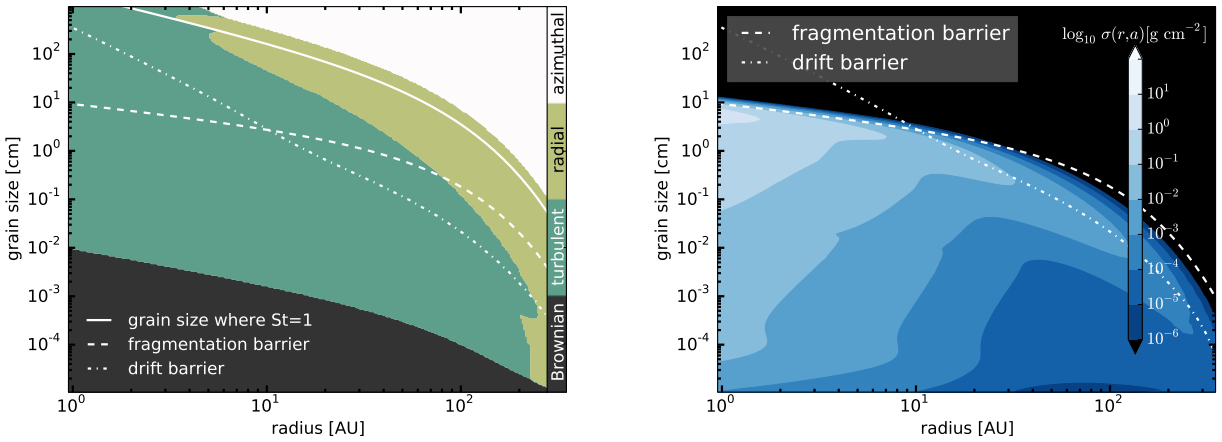

Fig. 3.— Left panel: important particle sizes and regimes of relative velocities in a fiducial disk model. The solid white line denotes the particle size corresponding to a Stokes number of unity, i.e. the fastest drifting dust particles. The dashed and dash-dotted lines are the size barriers due to fragmentation and radial drift, respectively (see Eqs. 8 and 9). The colored areas denote the dominating source of relative velocities at a given particle size and radius. This plot used a disk mass of 1% of the stellar mass, a stellar mass of 1 $M_\odot$, a turbulence parameter α_t of 1×10^{-3}, a fragmentation velocity of 3 m s^{-1}, a solid density of 1.6 g cm^{-3}, and a self similar gas surface density (see *Lynden-Bell and Pringle*, 1974) with viscosity index p=1 and characteristic radius of 60 AU, and a temperature profile of $T = 50K(r/10\ \mathrm{AU})^{-0.5}$. Right panel: grain size distribution as a function of radius on the disk after 3×10^6 years for the same parameters as above. The initial dust-to-gas ratio is 10^{-2}, but the resulting dust-to-gas ratio at 3 Myrs was used in the left panel.

in velocity. In the case of a massive disk, the entire dust population is lost towards the inner boundary. Similar results were found by *Laibe et al.* (2008), who implemented the growth prescription of *Stepinski and Valageas* (1997) into an SPH code.

Garaud (2007) extended upon this idea by assuming the particle size distribution to be a MRN-like power-law (see, *Mathis et al.*, 1977) up to a certain maximum size. The maximum size was assumed to evolve as it sweeps up other grains but the small grains were not evolved accordingly, i.e. they were assumed to be produced by fragmentation, even though fragmentation was not taken into account. This way, similar to previous works, particles could grow unhindered to planetesimals. One important finding of *Garaud* (2007) was that the dust mass in the outer disk represents a reservoir for the inner disk. As the small grains in the outer disk grow, they start to spiral inwards due to radial drift and feed the inner disk.

Another approach was taken by *Birnstiel et al.* (2012), where results of full numerical simulations (see Sect. 4.4) were taken as a template for a simplified model. In this model, the dust distribution is divided into small grains, which are basically following the gas motion, and large grains which contain most of the mass and are subject to significant radial drift. The full numerical results showed that the shape and upper limit of the size distributions mostly represent two limiting cases, where either radial drift or grain fragmentation is the size limiting factor. The resulting grain size yields an effective transport velocity that can be used to calculate the evolution of the surface density, which agrees well with the full numerical solutions.

4.4. Detailed global dust evolution models

The first models treating both the dust collisional evolution and radial transport in a protoplanetary disk were done by *Schmitt et al.* (1997) and *Suttner and Yorke* (2001), however these works could only simulate the evolution for 100 and 10^4 years, respectively. Still, they already showed that especially in the innermost regions, grain growth is occurs very quickly and that the initial growth is driven by Brownian motion until turbulence induced relative velocities dominate at larger sizes.

The models of *Dullemond and Dominik* (2005) and *Tanaka et al.* (2005) were global in the sense that they simulated dust evolution and vertical transport at several radial positions of the disk, thus being able to calculate spectral energy distributions of disk, but they did not include the radial transport.

The models of *Brauer et al.* (2008a) and *Birnstiel et al.* (2010a) were among the first to simulate dust evolution and radial transport for several millions of years, i.e. covering the typical life time of protoplanetary disks. This was possible by treating the dust evolution in a vertically integrated way, which reduces the problem to one spatial and the mass dimension. They showed that both radial drift and grain shattering collisions pose a serious obstacle towards the col-

lisional formation of planetesimals. *Brauer et al.* (2008b) used such a model to show that in the scenario of *Kretke and Lin* (2007), dust particles can accumulate in pressure bumps and form larger bodies, as long as turbulence is weak enough to avoid particle fragmentation.

A common feature of basically all simplified and full global models is the *radial drift barrier*, which limits the maximum size that particles can reach. Technically speaking, it is not a growth barrier, as it is not limiting the particle growth itself, but it still enforces an upper size cutoff by quickly removing particles larger than a particular size. Setting aside the other possible barriers and assuming particles perfectly sticking upon collision, we can define a growth time scale $t_{\rm grow} = a/\dot{a}$, which is the time scale on which the size is doubled. For a mono-disperse size distribution of spherical grains, the growth rate can be written as $\dot{a} = \Delta u\, \rho_{\rm dust}/\rho_{\rm s}$, where $\rho_{\rm dust}$ is the dust density and Δu the collision velocity. $\dot{a}$ can be thought of as the velocity of motion along the vertical axis in Fig. 3, while the radial drift velocity is the motion along the horizontal axis. The size limit enforced by drift is therefore approximately where the growth time scale exceeds the drift time scale $t_{\rm drift} = r/u_{\rm drift}$, which is approximately given by (see, *Birnstiel et al.*, 2012, and Fig. 3)

$$a_{\rm drift} \simeq 0.35 \frac{\Sigma_{\rm dust}}{\rho_{\rm s}} \frac{V_{\rm K}^2}{c_{\rm s}^2} \left| \frac{{\rm dln}P}{{\rm dln}r} \right|^{-1}. \quad (9)$$

Having most of the dust mass contained in the largest grains of a given size $a_{\rm max}(r)$, the transport velocity of the dust surface density can roughly be approximated as $u_{\rm drift}(a_{\rm max}(r))$. In a quasi-stationary situation, where the dust is flowing inward at a rate $\dot{M}_{\rm dust}$, the surface density profile follows directly from the mass conservation

$$\Sigma_{\rm dust} = \frac{\dot{M}_{\rm dust}}{2\pi\, r\, u_{\rm drift}}. \quad (10)$$

If the largest grain size is set by fragmentation, which is mostly the case in the inner disk (cf. Fig. 3), then the dust surface density was shown to follow a profile of $\Sigma_{\rm dust} \propto r^{-1.5}$, which is in agreement with both the estimates for the solar system (*Weidenschilling*, 1977; *Hayashi*, 1981) and the estimates from extrasolar planets of *Chiang and Laughlin* (2013).

If radial drift is at play, and the dust surface density drops, then particularly the outer disk will at some point become dominated by the radial drift barrier, in which case the resulting dust surface density profile was shown to be $\Sigma_{\rm dust} \propto r^{-(2p+1)/4}$ (where $\Sigma_{\rm gas} \propto r^{-p}$), in agreement with current observations of *Andrews et al.* (2012).

A possible way of overcoming the drift barrier, however for a limited spatial range, was discussed in *Okuzumi et al.* (2012). They used the method of *Okuzumi et al.* (2009) to simulate the porosity evolution in addition to the global evolution of non-fragmenting dust particles, based on a collisional model of *Suyama et al.* (2012). They found that outside the snow line, but inside of around 10 AU, extremely porous particles, as formed in this collisional model (internal densities of the order of 10^{-5} g cm^{-3}), have a strongly decreased growth time due to their increased collisional cross section, which allows them cross the drift barrier. Sintering (e.g. *Sirono*, 2011a,b) is expected to prevent this mechanism inside approximately 7 AU (*Okuzumi et al.*, 2012). However, the precise impact that sintering, or fragmentation has on this mechanism remains to be investigated.

4.5. Summary: Modeling

Current modeling efforts are standing on the proverbial shoulders of giants: laboratory work, numerical modeling of individual particle collisions, and theoretical studies on disk structure, turbulence, collision velocities, and other physical effects represent the foundation on which global models of dust evolution are build.

Models predict grains to grow to different sizes, migrate and mix radially and vertically throughout the disk. Large grains are expected to settle on the mid-plane and be transported radially to the inner disk regions, while small grains are mixed vertically to the disk surface by turbulence and transported outwards as the gas spreads out as part of the disk viscous evolution. The growth timescale is also longer in the outer regions of the disk, as a consequence, this region acts as a reservoir for the inner disk. Dust evolution in the planet forming regions of the disk is strongly influenced by the rate at which large solids are transported inwards from the outer disk. Understanding how to slow down the radial transport is one of the important goals for the future research in this field.

Current models of non-fractal grain growth can explain the formation of larger bodies by incremental growth, but most of the dust mass tends to be trapped either by fragmentation or by radial drift. Size limits associated with these effects lead to a characteristic dust surface density distribution, that can be compared directly with observations (see § 8). Fractal dust aggregates with internal densities of the order of 10^{-5} – 10^{-3} g cm^{-3} experience accelerated growth and could break through the radial drift barrier. A detailed analysis of the evolution of these aggregates and their observational properties are an active area of research, where we also expect rapid progress in the coming years.

5. EFFECTS OF GRAIN GROWTH ON DUST OPACITY

The wavelength-dependent absorption and scattering properties of dust grains change as they grow in size. This behavior provides a tool to study the grain growth through panchromatic observations of circumstellar disks from optical to centimeter wavelengths.

A significant fraction of the disk emission at optical and

near-infrared wavelengths consists of stellar light scattered by the dust grains in the superficial layer of the disk (see Fig 1). The morphology and color of the scattered light is most sensitive to grains with sizes between 0.01-10 μm, which correspond to the transition between the Rayleigh and the Mie scattering. As a general trend, as grains grow the scattering phase function becomes more isotropic and the color of the scattered light turns redder (*Bohren and Huffman*, 1983). In addition, the strength of mineral spectroscopical features, e.g. the silicate resonance feature at 10 μm, decreases (see *Kessler-Silacci et al.*, 2006, and references therein). As discussed in § 7, spatially resolved and spectroscopic observations of disks allow therefore to measure the size of dust grains in the surface layer of the disk.

Observations at longer wavelengths probe the dust properties in the disk interior where most of the mass is located. From far-infrared to millimeter wavelengths, the disk emission is dominated by the thermal emission from warm dust which is controlled by the dust opacity κ_ν. For dust grains with minimum and maximum sizes a_{min} and a_{max}, a good approximation is a power law, $\kappa_\nu \propto \nu^\beta$, where the spectral index β is sensitive to a_{max} but does not depend on a_{min} for $a_{min} < 1\mu$m (*Miyake and Nakagawa*, 1993; *Draine*, 2006).

The dust opacity spectral index β does not depend only on the grain sizes of the emitting dust, but also on other factors such as dust chemical composition, porosity, geometry, as well as on the the grain size distribution, normally assumed as a power law of the form $dN = n(a)^{-q}da$ (e.g. *Natta et al.*, 2007). The main result is that, regardless of all the uncertainties on the dust model, dust grains with sizes of the order of 1 mm or larger lead to β values lower than about 1 (Fig. 4, see also *Natta and Testi*, 2004).

The inferred range of β values in young disks has also an important consequence on the derivation of dust masses through sub-mm/mm photometry, which implies knowledge of the dust opacity coefficient. Solids with sizes much larger than the wavelength of the observations do not efficiently emit/absorb radiation at that wavelength and are therefore characterized by low values of the dust opacity coefficient. Physical models of dust emission have been used to quantify the effect of changing β on the millimeter dust opacity coefficient. For example, for the dust models of *D'Alessio et al.* (2006) with a slope of 2.5 for the grain size distribution, a dust population with $\beta \approx 0.2$ has a dust opacity coefficient at 1 mm lower by nearly 2 orders of magnitude than a dust population with $\beta \approx 1.0 - 1.5$. This difference can be understood by the fact that, for a given slope of the grain size distribution, a value of β much lower than 1 requires extending the distribution to very large grains, much larger than the observing wavelength. Similar results are obtained with the dust models considered in *Ricci et al.* (2010b). Despite the fact that the absolute value of the dust opacity at any wavelength strongly depends on the adopted dust model, this shows how inferring relations which involve disk dust masses without accounting for possible variations of the β parameter throughout the sample can lead to potentially large biases and errors.

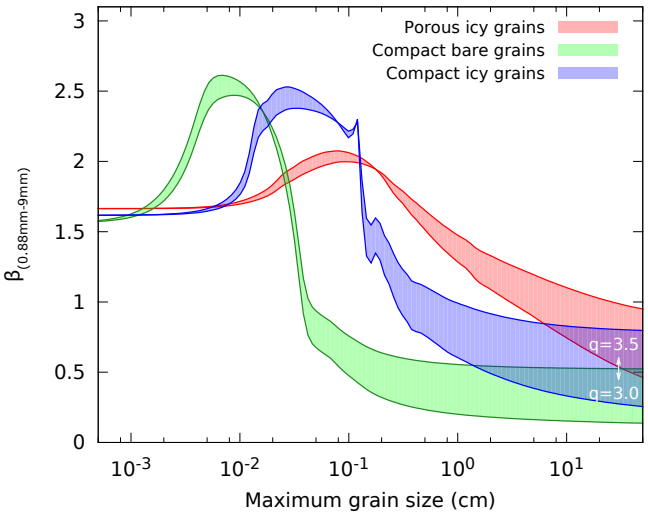

Fig. 4.— Spectral index β of the dust opacity $\kappa_\nu \propto \nu^\beta$ calculated between the wavelengths of 0.88 mm and 9 mm as a function of the maximum grain size, for a grain size distribution $n(a) \propto a^{-q}$ characterized by a minimum grain size of 0.01 μm. Different colors corresponds to grains with different chemical composition and porosity. Red: grains composed by astronomical silicates, carbonaceous material, and water ice, with relative abundances as in *Pollack et al.* (1994) and a porosity of 50%. Blue: compact grains with the same composition as above. Green: compact grains composed only of astronomical silicates and carbonaceous material. For each composition, the colored region shows the values of β in the range $q = 3.0$ to $q = 3.5$. Despite the dependence of β on the grain composition and the value of q, maximum grain sizes larger than about 1 mm lead to values of β less than unity. This opacities have computed following the prescription as in *Natta and Testi* (2004).

6. DUST EVOLUTION BEFORE THE DISK FORMATION

This review focuses on the dust evolution in protoplanetary discs as the first step of the formation of planetesimals and larger bodies in planetary systems. Nevertheless, many of the physical processes described in the first two sections are also expected to occur in molecular cloud cores and in the envelopes of protostars before the disk formation stage.

Grain coagulation and growth in cores and protostellar envelopes have been modeled by several authors (e.g. *Ossenkopf*, 1993; *Weidenschilling and Ruzmaikina*, 1994; *Suttner et al.*, 1999; *Ormel et al.*, 2009). These models show that grains can form fluffy aggregates very efficiently as a function of core density and time. The growth is favored by the presence of ice mantles, which are expected to form in the denser and cooler interior of the clouds. Taking the most recent calculations by *Ormel et al.* (2009), on a timescale

of $\sim$1 Ma, grains can grow to several micron-size particles at densities of $\sim 10^5$ cm^{-3}, and reach several hundred micron size aggregates at higher densities. The effects of these changes on the dust scattering and absorption properties have also been computed and has been shown that the growth can be traced combining absorption, scattering and emission at different wavelengths (*Kruegel and Siebenmorgen*, 1994; *Ossenkopf and Henning*, 1994; *Ormel et al.*, 2011).

Detailed modeling of the infrared scattered light from dark cores in molecular clouds has shown widespread evidence for the presence of dust grains grown to several micron size particles, even in relatively low density regions (*Pagani et al.*, 2010; *Steinacker et al.*, 2010). This is consistent with the models described above if the cores survive for timescales of the order of $\geq$1 Ma. These findings are in agreement with studies of the optical and infrared extinction law in nearby molecular clouds (eg. *Foster et al.*, 2013). Evidence of growth to larger sizes in the densest regions of molecular cloud cores have been investigated by measuring the dust emission at far infrared and submillimeter wavelengths and comparing the emission properties with extinction in the optical and infrared (eg. *Stepnik et al.*, 2003; *Roy et al.*, 2013; *Suutarinen et al.*, 2013). Solid results in this context have proven elusive so far, the main limitations of the current studies are the sensitivity of wide area infrared surveys that do not see through the densest regions of cores. The use of the sub-millimeter spectral index as a probe of the grain size distribution has been questioned by several studies which showed a possible dependence of the dust opacity with temperature (*Paradis et al.*, 2010; *Veneziani et al.*, 2010). However, recent detailed studies of dense and cold clouds which include a broader range of (sub-)millimeter wavelengths, suggest that, in some cases, the observed anti-correlation between the dust opacity spectral index β and temperature may be the result of the uncertainties resulting from using simplified single temperature modified black body fits to observations covering a limited range of wavelengths (*Shetty et al.*, 2009; *Kelly et al.*, 2012; *Sadavoy et al.*, 2013; *Juvela et al.*, 2013). Indirect evidence supporting grain growth in the dense regions of pre-stellar cores has been obtained by *Keto and Caselli* (2008), which invoke significant grain growth at densities exceeding 10^5 cm^{-3} to explain the inferred change in dust opacity in the inner regions of the studied pre-stellar cores.

A recent development has been the study of dust properties in protostellar envelopes and young disks. The dust opacity index in the youngest protostars indicate possible evidence for large grains in the collapsing envelopes (*Jørgensen et al.*, 2009; *Kwon et al.*, 2009). These initial results have been recently followed up with better data and more detailed modeling, which confirmed the initial suggestion that $\beta \leq 1$ in the inner envelopes of the youngest protostars (*Chiang et al.*, 2012; *Tobin et al.*, 2013*Miotello, priv. comm.)*. These findings suggest that large dust aggregates, perhaps up to millimeter size, can form during the disk formation stage in the infalling envelopes and are broadly in agreement with a very fast formation of Calcium-Aluminum Inclusions in carbonaceous chondritic meteorites (*Connelly et al.*, 2012, see also the chapter by Johansen et al.).

7. CONSTRAINTS ON DUST GROWTH IN DISKS FROM NIR AND MIR OBSERVATIONS

Because of the impact of density on time scales for growth, it is clear that the major part of dust growth has to happen in the mid-plane of the disk, where densities are highest. The outer surfaces of the disk are mainly acting as display cases where products of this dust growth, more or less modified by transport processes from the mid-plane to the surface, are displayed to the observer by their interaction with optical, near and mid IR radiation. These surfaces are the upper disk surface, at the inner rim. The upper disk surface is relevant because it is directly illuminated (if the disk is flaring), and it also allows radiation at wavelengths well below the sub-mm regime to escape. As vertical mixing happens on time scales that are short compared to radial transport, grains in the disk surface are related to the population on the mid-plane at the same distance from the star. The inner rim of the disk is important because dust gets exposed, often at temperatures close to its evaporation temperature. The inner rim also allows in principle to study mid-plane dust by constraining the evaporation surface, the initial results show that grains larger than micron-size particles are required, but this avenue of research has so far been only marginally explored (e.g. *Isella et al.*, 2006; *Dullemond and Monnier*, 2010; *McClure et al.*, 2013).

The tracers of dust size at these surfaces are (i) Angular and wavelength dependence of scattered light, both intensity and polarization, and (ii) The shape and strength of dust emission features (*Dullemond and Monnier*, 2010).

7.1. Scattered light

Scattered light images can resolve the disks of nearby young stars down to distances of about 20AU (e.g. *Ardila et al.*, 2007) from the star, in some cases even down to about 10AU (*Quanz et al.*, 2012). Scattered light carries information about grain size in the intensity of the scattered light, and in particular in the angular dependence of the intensity, i.e. the phase function. The brightness of scattered light is often low, indicating grains with low albedo (*Ardila et al.*, 2007; *Fukagawa et al.*, 2010). The color of disks can be redder than that of the star (*Ardila et al.*, 2007; *Clampin et al.*, 2003; *Wisniewski et al.*, 2008), an effect that can be explained by the presence of large grains with wavelengths-dependent effective albedo caused by a narrowing of the forward-scattering peak at shorter wavelengths (*Mulders and Dominik*, 2012). Observed disks often differ in brightness between the front and back side (e.g. *Kudo et al.*, 2008), and a brighter front side is often taken as a sign for large grains whose scattering phase function is

dominated by forward scattering (*Quanz et al.*, 2011). However, *Mulders et al.* (2013) warn that large grains, if present in the disk surface, may have phase functions with a very narrow forward scattering peak of only a few degrees that can never be observed except in edge-on disks. The behavior of the phase function at intermediate angles (the angles actually seen in an inclined disk) may depend on details of the grain composition and structure.

Model fitting of scattered light images taken at multiple wavelengths indicate the presence of stratification, with smaller grains higher up in the disk atmosphere and larger grains settled deeper (e.g. *Pinte et al.*, 2007, 2008; *Duchêne et al.*, 2010), in accordance with the predictions of models (e.g. *Dullemond and Dominik*, 2004).

7.2. Dust features

The usefulness of mid-IR features as tracers of dust growth is limited because the spatial resolution currently available at these wavelengths makes it hard to study the shape of features as a function of distance from the star, so only an average profile is observed. Interferometric observations allow us to extract the spectrum emitted by the innermost few AU (*van Boekel et al.*, 2004), showing that the inner regions are much more crystallized than the disk integrated spectrum indicated. Pioneering work on the integrated spectrum with ISO on Herbig stars (*Bouwman et al.*, 2001; *van Boekel et al.*, 2005) has in recent years been extended to larger samples of Herbig stars, and to T Tauri stars, making use of the better sensitivity provided by Spitzer. The result of these studies is that grains of sizes around 1 to a few micrometers must form quickly as the resulting broadening and weakening of the 10 and 20 μm features are present in most disks, essentially independent of age and other stellar parameters (*Kessler-Silacci et al.*, 2006; *Furlan et al.*, 2006; *Juhász et al.*, 2010; *Oliveira et al.*, 2011). *Juhasz et al.* find that larger grains are more prominent in sources that show a deficit of far infrared emission, interpreted as an indication of a flatter disk structure. These findings are in apparent contraddiction with the results of *Sicilia-Aguilar et al.* (2007), who find an apparent trend for smaller grains in the atmospheres of older disks in Tr37. The interpretation for these observations is that larger grains settle more rapidly onto the midplane, as compared to small grains, and hence, at later ages, are not accessible to infrared observations. As infrared observations probe a thin surface layer of the disk at a radius that is a strong function of the central star parameters (eg. *Kessler-Silacci et al.*, 2007; *Natta et al.*, 2007), it is very difficult, and possibly misleading to use spatially unresolved spectroscopy as a probe of global dust growth in disks. Nevertheless, an important result shown by all these studies is that the dust producing the 10 and 20 micron features contains a significant fraction of crystalline material, indicating that this dust was heated to temperatures of around 1000 K during processing in the disk. *Ábrahám et al.* (2009) and *Juhász et al.* (2012) clearly detected the increased production and subsequent transport to the outer disk of crystalline dust during the 2008 outburst of the star EX Lup. These findings suggest that eruptive phenomena in young disk-star systems play an important role in the processing and mixing of dust in protoplanetary disks.

7.3. Constraints for mid plane processes

It is now generally believed that dust in the inner parts of the disk quickly develops into a steady-state situation with on-going coagulation and reproduction of small grains by erosion and fragmentation (see section 4.2). The dust present in the disk surface therefore does not seem to be a good tracer of the evolution of the mean and maximum particles size in the mid plane of the disk, but rather reports on the presence of this steady state. While an suggestion of a possible correlation between mid-plane and surface dust processing was made by *Lommen et al.* (2009), many previous and subsequent attempts based on larger surveys have so far shown a distinct lack of correlation (*Natta et al.*, 2007; *Ricci et al.*, 2010a; *Juhász et al.*, 2010), probably caused by the fact that mid infrared observations are tracing the atmosphere of the inner disk (0.1-10 AU depending on the stellar properties), while mid-plane dust has so far been probed only in the outer disk (beyond $\sim$ 20 AU, see § 8).

8. OBSERVATIONS OF GRAIN GROWTH IN THE DISK MID-PLANE

The denser regions of the disk mid-plane can be investigated at (sub-)millimeter and centimeter wavelengths, where dust emission is more optically thin. Long wavelength observations are thus the unique tool that allow us to probe grain evolution on the disk mid-plane, where most of the mass of the solids is confined and where planetesimal and planet formation is thought to occur. In this section we will focus on the observational constraints on grain growth on the disk mid-plane from long wavelength observations, describing the methodology and limitations of this technique (§ 8.1) as well as the results of the relatively extensive photometric surveys (§ 8.2) and of the more limited, but very promising for the future, spatially resolved multi-wavelength observations (§ 8.3).

8.1. Methodology

As described in § 5, as grains grow to sizes comparable with the observing wavelength, the dust opacity changes significantly, imprinting the signature of growth in the disk emission. In particular, at millimeter and centimeter wavelengths, the spectral index of the emission of optically thin dust at a given temperature can be directly related to the spectral dependence of the dust opacity coefficient, which in turn is related to the maximum grain size.

Values of β for dust in proto-planetary disks can be derived by measuring the slope $\alpha_{\rm mm}$ of the sub-mm SED ($F_\nu \propto \nu^{\alpha_{\rm mm}}$). Under the simple assumptions of optically

thin dust emission in the Rayleigh-Jeans tail of the spectrum, then $\beta = \alpha_{\rm mm} - 2$. The first single-dish and interferometric observations which measured the sub-mm slope of the SED of young disks came in the late 80s and early 90s (*Weintraub et al.*, 1989; *Woody et al.*, 1989; *Adams et al.*, 1990; *Beckwith and Sargent*, 1991). These pioneering works already revealed a wide interval of β-values ranging from ≈ 0 up to the values typical of the ISM (≈ 1.7). The presence of dust grains with sizes larger than about 0.1 mm was soon recognized as a possible explanation for the disks showing $\beta < 1$ (*Weintraub et al.*, 1989; *Beckwith and Sargent*, 1991).

While this simplified approach has been useful in the initial studies, it is obvious that it has serious limitations and should not be used now that quick and efficient programs to self consistently compute the dust emission from a protoplanetary disk with an arbitrary dust opacity are fast and widely available. All the results that we present in this chapter are derived using disk models that include an approximate, but proper treatment of the density and temperature profile in the disk and use opacities computed from physical dust models (e.g. *Chiang and Goldreich*, 1997; *Dullemond et al.*, 2001, 2007; *Natta and Testi*, 2004, and successive improvements). These models include an approximate treatment of the radiation transfer in the regions where the disk becomes optically thick even at millimeter wavelengths under the assumption of a smooth disk structure. The effect of including optically thick regions due to local over-densities at large distances from the star has been investigated and shown to be unlikely to play a major role in protoplanetary disks by *Ricci et al.* (2012b). Another serious source of uncertainty, if proper disk emission models are not considered, comes from the assumption that the whole disk emission is in the Rayleigh-Jeans regime, as the dust temperature in the outer disk mid-plane easily reach values below 15-20 K. Neglecting the effects of optical depth and of the low dust temperatures can result in a significant underestimate of β, leading to incorrect results on grain growth (see e.g. *Weintraub et al.*, 1989; *Testi et al.*, 2001, 2003; *Wilner et al.*, 2005).

Another aspect to be considered is whether other sources of emission might be contaminating the signal from the large grains at the observing wavelengths. The major source of uncertainties comes from the contamination of the emission at long wavelength from gas in the stellar chromosphere or in the wind/jets. The typical approach used to resolve this uncertainty is to combine the millimeter observations with long wavelength observations that probe the gas emission (*Testi et al.*, 2001, 2003; *Wilner et al.*, 2005; *Rodmann et al.*, 2006). All these studies show that for T Tauri stars, not affected by intense external photoionization, the contribution of the gas emission at wavelength shorter than 3 mm is below the 30% level. It is important to note that this is an estimate and, especially for the fainter disks and the higher mass central stars the contribution may be significantly higher and need to be accounted properly. In regions where there is a strong external ionizing radiation, the contribution of the gas to the emission may be dominant at 3mm and still be significant at 1mm. An example of this condition are the inner regions of the Trapezium cluster in Orion (e.g. *Williams et al.*, 2005; *Eisner et al.*, 2008; *Mann and Williams*, 2010, and references therein). Since non-thermal emission and thermal free-free from an ionized wind vary on various time-scales (e.g. *Salter et al.*, 2010; *Ubach et al.*, 2012, and references therein), nearly simultaneous observations at (sub-)mm and cm wavelengths should be used to quantify the gas spectrum and subtract it from the measured fluxes to infer the emission from dust only.

8.2. Results from multi-wavelegth sub-mm photometry

Natta et al. (2007) covered the main results obtained in this field until the first half of the last decade. The main conclusion at the time was that, while evidence for large grains had been found in several bright disks, no clear trend with the properties of the system or age was evident. Since then, many photometric surveys have targeted young disks in several nearby star forming regions (distances < 500 pc from the Sun) at long wavelengths, with the goal of constraining dust evolution in less biased samples.

The most extensive studies aimed at a derivation of the grain growth properties have been performed for the Taurus-Auriga (*Andrews and Williams*, 2005; *Rodmann et al.*, 2006; *Ricci et al.*, 2010b) and Ophiuchus *Andrews and Williams* (2007); *Ricci et al.* (2010a) star forming regions. Less extensive studies have also been carried out in southern star forming regions (*Lommen et al.*, 2009; *Ubach et al.*, 2012) and the more distant Orion Nebula Cluster (*Mann and Williams*, 2010; *Ricci et al.*, 2011). It is important to note that all the surveys of disks conducted to date with the aim of characterizing the spectral index β of the dust absorption coefficient are far from being complete in any star forming region, and the level of completeness decreases with decreasing disk mass. In many cases the studies included a detailed analysis of the possible contribution of the gas emission at long wavelengths and enough resolution to confirm that the disks are mostly optically thin and, for the large part, followed the methodology described in § 8.1 to derive the level of grain growth.

Following the method laid out by *Ricci et al.* (2010b), we have selected a subsample of all the published measurements of the 1.1–3 mm spectral index for disks surrounding single stars (or wide separation binaries) of spectral type from K and early M. The measured spectral indices are plotted in Fig. 5 against the flux measured at 1.1 mm (scaled at a common distance of 140 pc). The flux is roughly proportional to the total dust mass in the disk (assuming similar dust properties in all disks).

The main results of these surveys is that the dust in the outer disk regions appears to have grown to sizes of at least

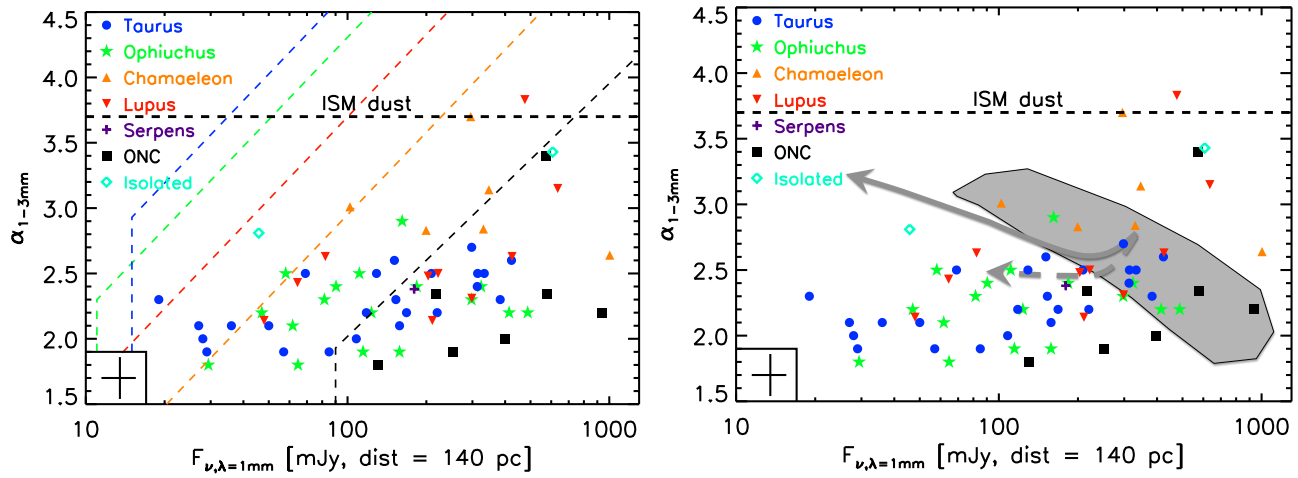

Fig. 5.— Left panel: Spectral index between 1.1 and 3 mm plotted against the flux at 1.1 mm (scaled for a common distance of 140 pc) for disks around single stars (or wide binaries) with spectral types early M to K in nearby star forming regions. The dashed lines mark the typical sensitivity limits of the surveys in Taurus, Ophiuchus, Lupus, Chamaeleon and Orion Nebula Cluster. Right panel: The grey area illustrate the range of predictions for global dust evolution models without radial drift (*Birnstiel et al.*, 2010b), the two arrows illustrate the evolutionary trajectories in the first few million years as predicted by the global models including the effect of radial drift (solid line) and including pressure traps in the gas distribution to slow the rate of drift (dashed line, *Pinilla et al.*, 2012b).

$\sim$ 1 mm for the vast majority of the disks. Within the relatively small samples investigated so far, the distribution of spectral indices is consistent with being the same for nearly all the regions probed so far. The general picture that is emerging from this comparison is that dust appears to quickly grow to large sizes, but then it needs to be retained in the disk for a relatively long time, comparable to the disk lifetime. The only region where there may be a hint for possibly different distribution of spectral index values is Chamaeleon, where *Ubach et al.* (2012) derived a range of β values between 0.9 and 1.8 for 8 disks. Chamaeleon is among the oldest regions in the sample (albeit still young with an estimated median age of $\sim$ 2 Ma *Luhman*, 2007). It is possible that the different values of α in Chamaeleon could be an indication for a time evolution of the grain size distribution, with a loss of mm/cm sized pebbles relative to smaller grains. This suggestion will be tested when statistically significant samples in younger and older star forming regions are observed with ALMA.

Following *Birnstiel et al.* (2010b) and *Pinilla et al.* (2012b), we show in Fig. 5 the prediction of global grain evolution models in disks. *Birnstiel et al.* (2010b) found that the measured 1.1–3 mm spectral indices can be well reproduced by models with reasonable values for parameters regulating grain fragmentation, gas turbulence and disk structure. However, these models are able to explain only the upper envelope of the measured fluxes (i.e. the most massive disks in the sample). There is a large population of disks that are difficult to reconcile with the model predictions: those with low millimeter flux and low spectral index (low-mass disks containing a substantial amount of large grains). This discrepancy cannot be solved by simply reducing the mass of the disk models, as disks with lower surface densities would hardly grow grains (*Birnstiel et al.*, 2010b), as can be seen by the fragmentation and drift limited growth in Equations 8 and 9, which show that the maximum grain size depend on the dust and gas surface density, respectively.

Pinilla et al. (2012b) investigated the effect of time evolution on these modeling results, finding that while the radial drift process would progressively reduce the disk mass, evolving over a few Ma the models to lower 1 mm fluxes, the drift and fragmentation processes will more efficiently remove the large grains from the disk, resulting in a steep increase of α which would not be consistent with the observations. *Pinilla et al.* (2012b) showed that the drift of large particles needs to be slowed down, but not halted completely, in order to explain the observed distribution in a framework of disk evolution. In this context, it is important to point out that no correlation has so far been found between individual stellar ages and α (e.g. *Ricci et al.*, 2010a).

Several mechanisms have been proposed to slow down the radial drift of large grains. For example in MHD simulations of disks with zonal flows (*Johansen and Klahr*, 2005; *Johansen et al.*, 2009; *Uribe et al.*, 2011), the pressure field in the disk would be modified and this may be a viable mechanism to create local pressure maxima that could efficiently trap large grains. Another possibility that has been explored by some authors is that very large grains are injected very early in the outer disk, then their migration is impaired as they are decoupled from the gas (e.g. *Laibe et al.*, 2012). This scenario would require the forma-

tion of very large (cm-size) grains in cores and protostellar envelopes before disk formation, or an extremely efficient growth in very massive (young) disks. These hypothesis have not yet been modeled in detail to explore their feasibility.

An important prediction of models of dust evolution in gaseous disks is that grains are expected to grow to a maximum size that depends on the local density of gas and dust (e.g. *Birnstiel et al.*, 2009). Therefore, larger values for the mm spectral indices should be expected for disks with lower flux at 1 mm, i.e. lower mass in dust and presumably lower densities as well. An extreme example of such systems could be disks around young brown dwarfs, if they are sufficiently large that the surface density is low. Initial measurements of these systems have confirmed the presence of large grains and relatively large radii (*Ricci et al.*, 2012a, 2013). In spite of the very low millimeter fluxes and estimated low dust mass, the mm spectral indices measured for the disks of $\rho-$Oph 102 and 2M0444+2512 are as low as for the bulk of the T Tauri stars, taken together with the information on the disk spatial extent from the interferometric observations *Ricci et al.* (2012a, 2013) constrain a value of $\beta \approx 0.5$ for both these brown dwarf disks.

Pinilla et al. (2013) and *Meru et al.* (2013) have investigated in detail the grain growth process in brown dwarf disks, showing that it is indeed possible to have grain growth and explain the values of millimeter flux and spectral index, at least in the conditions derived for the disks that have been observed so far. A more serious problem is represented by the radial drift. To slow down the radial motion of the grains *Pinilla et al.* (2013) had to assume rather extreme gas pressure inhomogeneities. ALMA will soon start to offer more observational constraints on larger samples of brown dwarf disks, allowing a more thorough test of the grain growth models.

8.2.1. Evolution of sub-mm fluxes for disks in different star forming regions

Additional evidence for dust grain growth comes from (sub-)millimeter continuum surveys of star forming regions with different ages. The key finding is that the disk millimeter luminosity distribution declines rapidly with time, much quicker than the infrared fraction, such that very few disks are detected at all in regions older than a few Ma.

The Taurus and Ophiuchus clouds host two of the best studied, nearby, low mass star forming regions and provide a benchmark for comparisons with other regions. Each contains about 200 Class II sources that have been well characterized at infrared wavelengths through Spitzer surveys (*Evans et al.*, 2009; *Luhman et al.*, 2010). Almost all these sources have been observed at (sub-)millimeter wavelengths in Taurus (*Andrews et al.*, 2013, and references therein) and a large survey was carried out in Ophiuchus by *Andrews and Williams* (2007). Both regions are relatively young, in the sense of having an infrared disk fraction, $f_{\rm disk} = N_{\rm disk}/N_{\rm tot} \geq 60\%$ and the disk millimeter distributions are broadly similar, lognormal with a mean flux density mean $F(1.3\,{\rm mm}) = 4\,{\rm mJy}$ and standard deviation 0.9 dex (*Andrews et al.*, 2013).

However, only a handful of disks are detected at millimeter wavelengths in more evolved regions such as Upper Sco ($f_{\rm disk} = 19\%$, *Mathews et al.*, 2012) and σ Ori ($f_{\rm disk} = 27\%$ *Williams et al.*, 2013). Statistical comparisons must take into account not only the varying survey depths of course, but also the stellar properties of the samples as disk masses depend on both stellar binarity and mass (*Andrews et al.*, 2013). The results of a Monte-Carlo sampling technique to allow for these effects demonstrates that infrared Class II disk millimeter luminosities decrease significantly as regions age and $f_{\rm disk}$ decreases (*Williams et al.*, 2013).

The precise ages (and age spreads) of the compared regions are not well known but they are all young enough, $\ll 10\,{\rm Myr}$, that planet formation should be ongoing. Therefore, the decrease in millimeter luminosity is attributable more to a decrease in the emitting surface area per unit mass, i.e., grain growth, than a decrease in the solid mass (*Greaves and Rice*, 2010). The relative age differences of Upper Sco and σ Ori with respect to Taurus are better constrained and are $\sim 3-5\,{\rm Myr}$. This is, therefore, an upper limit to the typical timescale on which most of the solid mass in disks is locked up into particles greater than about a millimeter in size.

8.3. Resolved Images at Millimeter/Radio Wavelengths

The theoretical models for the evolution of solid particles in protoplanetary disks that were described in §4 make several physical predictions that should have direct observational consequences: (1) settling, growth and inward drift conspire to produce a size-sorted vertical and radial distribution of solids, such that larger particles are preferentially more concentrated in the disk mid-plane and near the host star; (2) drift alone should substantially increase the gas-to-dust mass ratio at large disk radii (especially for mm/cm-sized particles); and (3) dust transport and fragmentation processes imply that the growth of solids to planetesimals has to happen in spatially confined regions of the disks. With their high sensitivity to cool gas and dust emission at a wide range of angular scales, observations with mm/radio-wavelength interferometers are uniquely suited for an empirical investigation of these physical effects. Ultimately, such data can be used to benchmark the theoretical models, and then provide observational constraints on their key input parameters (e.g. turbulence, particle properties, growth timescales, etc.; see §3 and 4).

8.3.1. Constraints on large scale radial variation of dust properties in disks

In the context of the dust continuum emission, we already highlighted in §8.2 how the disk-averaged mm/radio "color" – typically parameterized in terms of the spectral index of the dust opacity, β – provides a global view of

the overall level of particle growth in the disk. While this is a useful and efficient approach to study the demographics of large surveys, it cannot tell us about the expected strong spatial variations of the dust properties in individual disks (e.g. *Birnstiel et al.*, 2010b). A more useful technique would be to map out the spatial dependence of the mm/radio colors, $\beta(r)$ or its equivalent, by resolving the continuum emission at a range of observing wavelengths. The underlying principle behind this technique rests on the (well justified) assumption that the continuum emission at sufficiently long wavelengths is optically thin, so that the surface brightness profile scales like

$$I_\nu(r) \propto \kappa_\nu \, B_\nu(T) \, \zeta \, \Sigma_g, \tag{11}$$

where κ_ν is the opacity spectrum, $B_\nu(T)$ is the Planck function at the local temperature, ζ is the inverse of the gas-to-dust mass ratio, and Σ_g is the gas surface density profile – each of which is thought to vary spatially in a given disk.

The spectral behavior in Eq. (11) has been exploited to interpret multi-wavelength resolved continuum images in two basic approaches. The first approach acknowledges that the forward-modeling problem is quite difficult, since we do not really have an a priori parametric model for the spatial variations of κ_ν, T, or Σ_d (where the dust surface density profile, $\Sigma_d = \zeta \, \Sigma_g$). *Isella et al.* (2010) reasoned that, for a suitable assumption or model of $T(r)$, the spectral gradient of the surface brightness profile itself should provide an empirical measurement of the resolved mm/radio color regardless of Σ_d. In essence, parametric fits for the optical depth profiles at each individual wavelength, $\tau_\nu(r) \approx \kappa_\nu \Sigma_d$, can be converted into an opacity index profile,

$$\beta(r) = \frac{\partial \log \kappa_\nu(r)}{\partial \log \nu} \approx \frac{\partial \log \tau_\nu(r)}{\partial \log \nu}. \tag{12}$$

Although the initial studies that adopted this approach had insufficient data to conclusively argue for a non-constant $\beta(r)$, they did establish an empirically motivated technique that provides a straightforward means of mapping mm/radio colors (e.g. *Isella et al.*, 2010; *Banzatti et al.*, 2011). Put simply, this approach allows one to reconstruct the $\beta(r)$ required to reconcile seemingly discrepant continuum emission structures at different observing wavelengths.

A slight variation on this approach is to adopt a more typical forward-modeling technique, where an assumption is made for a parametric formulation for both κ_ν and Σ_d. For example, *Guilloteau et al.* (2011) explored their dual-wavelength observations of Taurus disks with power-law and step-function $\beta(r)$ profiles, and argued that a spectral index that increases with disk radius provides a substantially improved fit quality compared to a global, constant index. In a recent refinement of the *Banzatti et al.* (2011) work, *Trotta et al.* (2013) have developed a more physically motivated prescription for $\kappa_\nu(r)$ (parameterized as a function of the local grain size distribution) that clearly calls for an increasing $\beta(r)$ in the disk around CQ Tau.

In these initial studies, the fundamental technical obstacle was really the limited wavelength range over which sensitive, resolved continuum measurements were available (typically $\lambda = 1.3$–2.7 mm). An extension of this work to centimeter wavelengths offers a substantially increased leverage on determining $\beta(r)$ and uniquely probes the largest detectable solid particles, while also overcoming the systematic uncertainties related to the absolute amplitude calibration for individual datasets. In two recent studies of the disks around AS 209 (*Pérez et al.*, 2012) and UZ Tau E (*Harris, priv. comm.*), resolved continuum emission at $\lambda \approx 9$ mm from the upgraded Jansky Very Large Array (VLA) was folded into the analysis to provide robust evidence for significant increases in their $\beta(r)$ profiles (as shown together in Figure 6). The analysis of the $\beta(r)$ profiles, as inferred from the optical depth profiles, for these two objects suggest at least an order of magnitude increase in particle sizes when moving in from $r \approx 100$ AU to $\sim$10 AU scales.

Taken together, these multi-wavelength interferometric dust continuum measurements reveal a fundamental, and apparently general, observational feature in young protoplanetary disks: the size of the dust emission region is anti-correlated with the observing wavelength. The sense of that relationship is in excellent agreement with the predictions of theoretical models for the evolution of disk solids, where the larger particles that emit more efficiently at longer wavelengths are concentrated at small disk radii due to the combined effects of growth and drift. The quantitative characterization of this feature in individual disks is just getting started, but the promise of a new opportunity to leverage current observing facilities to constrain planetesimal formation in action is exciting. However, there is a downside: it is now clear that resolved observations at a single mm/radio wavelength are not sufficient to constrain fundamental parameters related to the dust density structure. Given the lingering uncertainty on an appropriate general parameterization for Σ_d, it is worthwhile to point out that the optimized mechanics of the modeling approach for these resolved multi-wavelength continuum data are still in a stage of active development. Yet, as more data becomes available, rapid advances are expected from both the theoretical and observational communities.

The behavior of the multi-wavelength dust continuum emission makes a strong case for the spatial variation of κ_ν induced by the growth and migration of disk solids. But, as mentioned at the start of this section, those same physical processes should also produce a complementary discrepancy between the spatial distribution of the gas and dust phases in a disk: the dust should be preferentially more concentrated toward the stellar host, and ζ should decrease dramatically with radius as the gas-to-dust ratio increases in the outer disk. The fundamental problem is that the derived dust densities are very uncertain, and, even more severe, we do not yet really understand how to measure gas densities in these disks, so we cannot infer $\zeta(r)$ with sufficient quan-

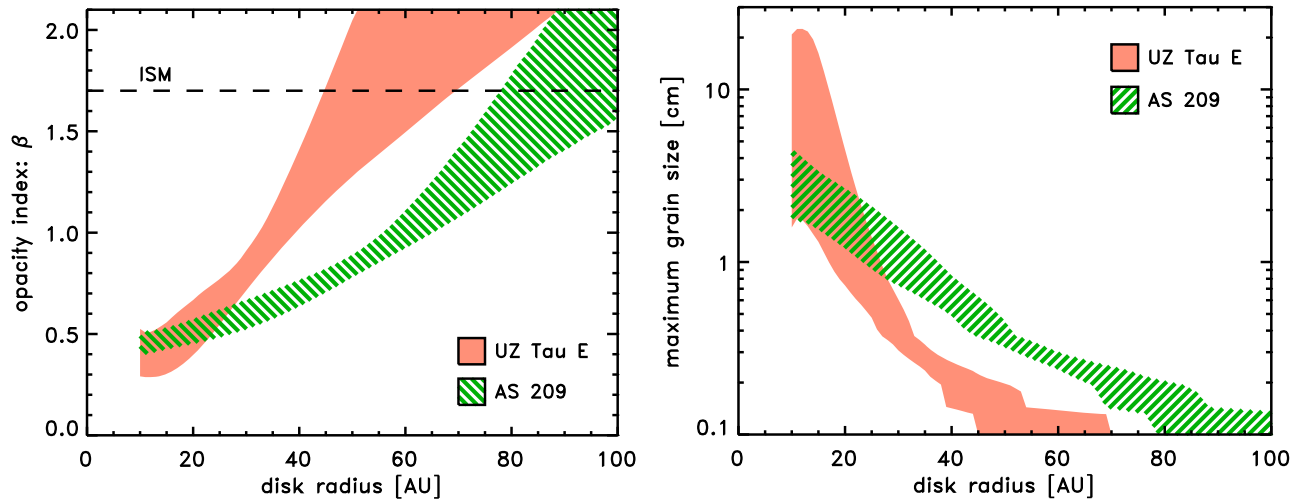

Fig. 6.— Left panel: confidence ranges for the profiles of β as a function of radius for the two disks surrounding the young stars AS 209 and UZ Tau E, as derived from sub-millimeter through centimeter wave high signal to noise and high angular resolution interferometric observations (*Pérez et al.*, 2012, *Harris, priv. comm.*). Right panel: values of a_{max} as a function of radius for the AS 209 and UZ Tau E disks derived with our reference dust model. The dashed and continuos lines show the fragmentation and radial drift limit, respectively, for a representative global model of dust evolution in disks (§ 4).

titative reliability.

However, an approach that relies on a comparison between the spatial extents of molecular line and dust continuum emission can provide an indirect constraint on the spatial variation of $\zeta(r)$, even if its normalization remains uncertain. It has been recognized for some time that the sizes of the gas disks traced by optically thick CO line emission appear systematically larger than their optically thin dust continuum (e.g. *Piétu et al.*, 2007; *Isella et al.*, 2007). Although previous work suggested that this may be an artificial feature caused by optical depth effects or a misleading density model (*Hughes et al.*, 2008), the CO–dust size discrepancies have persisted with more sophisticated models and improved sensitivity. The evidence for a decreasing $\zeta(r)$ profile is derived through a process of logical negation. First, the dust structure of an individual disk is modeled, based on radiative transfer calculations that match the broadband SED and one or more resolved continuum images. Then, a gas structure model is calculated assuming a spatially invariant ζ. A comparison of the corresponding synthetic CO emission model and the data invariably demonstrates that the model produces line emission that is much too compact. Small grains are found to be well mixed with the gas out to very large radii, e.g. from scattered light observations (see § 7). These findings imply that the large grains are confined to a smaller region of the disk, as compared to the gas and small dust grains. It is reasonable to deduce that a combination of grain size radial segregation and a decreasing $\zeta(r)$ would reconcile the line and continuum data.

As of this writing, only 5 disks have been modeled in this manner to indirectly infer a decreasing $\zeta(r)$, around IM Lup (*Panić et al.*, 2008), TW Hya (*Andrews et al.*, 2012), LkCa 15 (*Isella et al.*, 2012), V4046 Sgr (*Rosenfeld et al.*, 2013), HD 163296 (*de Gregorio-Monsalvo et al.*, 2013). Ultimately, an empirical measurement of the CO–dust size discrepancy could be combined with the $\beta(r)$ profile inferences to help better constrain drift rates and how the migration of solids depends on the local disk conditions.

8.3.2. *Constraints on vertical stratification of dust properties in disks*

In § 7 we discussed the important constraints that infrared and scattered light observations provide on the grain populations in the disk atmosphere and on the dust settling (an extensive discussion of these can also be found in *Natta et al.*, 2007). The initial attempts to relate the grain properties in the disk atmosphere, as derived from mid infrared spectroscopy, with the properties on the mid-plane, as derived from (sub-)millimeter photometry, have met very limits success, even when considering large samples (e.g. *Lommen et al.*, 2009; *Ricci et al.*, 2010a; *Juhász et al.*, 2010; *Ubach et al.*, 2012). While models do predict a relationship between the growth level on the mid-plane and the atmosphere of the disks, the atmosphere grains should reach a steady state balance between growth and fragmentation while mid-plane dust is still growing, in addition another likely cause of the difficulty in recovering a correlation between the dust properties observationally is most likely linked to the vastly different regions of the disks that are currently sampled in the two wavelength regimes (e.g. *Natta et al.*, 2007). A meaningful comparison will only be possible with data sampling the same regions of the disk, which will require substantial improvement of the mid-infrared observations, both in terms of sensitivity and angular resolution, which will become possible with the 40-

m class ELTs.

Better results are being obtained by comparing the dust properties as derived from high angular resolution optical-infrared images and millimeter dust emission maps. Constraints on the dust settling in the upper layers of the disk atmosphere have been discussed extensively in the last decade (§7 and, e.g.*Wolf et al.*, 2003, 2008, 2012; *Liu et al.*, 2012), so far, the main limitation to combined multi-wavelength studies that could constrain dust properties across the whole disk scale height has been the limited sensitivity and angular resolution of (sub-)millimeter observations. Some initial studies in this direction are promising, although these are currently limited to very few objects and with very favorable viewing geometries (e.g. *Gräfe et al.*, 2013). It is expected that ALMA will provide the angular resolution and sensitivity to significantly progress in this area, although, obviously, the best constraints will continue to be possible only for disks with very favorable geometries (*Boehler et al.*, 2013).

8.3.3. Constraints on small scale variation of dust properties and dust trapping

One key development that is expected in the near future is the direct observation of the expected small scale structures within the disk where solids will be able to overcome the many growth barriers discussed in §3 and 4 and reach the planetesimal stage (see also the chapter by Anders et al.). All of the proposed solutions to the long standing m-size barrier problem in planet formation (*Weidenschilling*, 1977, and all subsequent evolutions) involve the confinement of the largest particles in localized areas of the disk where they can locally overcome the barriers on their way to become planetesimals. The typical dimensions of these large grains "traps", as they are normally referred to, is of the order of the local scale height of the disk or less. Several studies have simulated in detail the observability of these features in young protoplanetary disks with ALMA showing that there are good prospects to reveal them both in the gas and/or dust emission (e.g. *Cossins et al.*, 2010; *Pinilla et al.*, 2012b, 2013; *Douglas et al.*, 2013).

A very recent and extremely encouraging development in this direction is the detection with ALMA of a large dust trap in a transition disk by *van der Marel et al.* (2013). These authors revealed clearly the segregation of large dust particles in the outer regions of the disk caused by the radial and azimuthal inhomogeneity in the gas density induced by the likely presence of a planetary companion within the disk inner hole. These data provide a direct observational support to the simulations of dust trapping in transitional disks as discussed by *Pinilla et al.* (2012a). While the result of *van der Marel et al.* (2013) provide a direct proof of the dust trapping concept, the characteristics of the observed system are such that the trap may support the formation of an analog to the Solar System Kuiper-Belt, but cannot obviously explain the formation of planets in that system, as the presence of a planet is a requirement for the formation of the trap. Nevertheless, the result illustrates how we can expect to constrain dust trapping in disks with ALMA in the future.

Sensitive and high angular resolution observations with ALMA will also very soon allow us to understand the role of snowlines in the evolution of solids in protoplanetary disks. Grains that are migrating inward across a snowline will loose part of their icy mantles and models predict that the cycle of sublimation and condensation will allow efficient growth and trapping across the snowline (e.g. *Ros and Johansen*, 2013). *Mathews et al.* (2013) and *Qi et al.* (2013) resolved spatially the CO snowline in HD 163296 and TW Hya, paving the road for an investigation of the role of this particular snowline in the evolution of solids.

9. SUMMARY AND OUTLOOK

Global models of grain evolution in disks, constrained by the results of laboratory and numerical calculations of grain and aggregate collisions, predict that in the conditions of protoplanetary disks grains should very rapidly grow to centimeter sizes. The growth process is not without difficulties, with numerous "barriers" to overcome. At this time, the most critical problem seems to be the drift-fragmentation "barrier" caused by the large differential radial speeds of grains of different sizes induced by the aerodynamical drag. While the level of growth predicted by models is consistent with observational data, the time evolution is too fast unless large grains radial drift motion is slowed down in pressure "traps". Several ideas of plausible mechanisms to produce these traps exist: from disk instabilities to snowlines. The predictions should now be tested observationally and ALMA will offer a unique opportunity to do this in the coming years thanks to its superb angular resolution and sensitivity.

Observations show that the majority of disks around isolated pre-main sequence stars in the nearby star forming regions contain a significant amount of grains grown to at least millimeter sizes. No clear evolutionary trends have emerged so far, although some indirect evidence of disk aging is starting to emerge also from millimeter observations. This finding strongly supports the notion that grain growth is a common and very fast process in disks, possibly occurring in the earliest phases of disk formation. The other implication is that the large grains are either kept in the disk mid-plane or they are continuously reformed for several Ma. This is required to explain the presence of these dust aggregates in disks around pre-main sequence stars and also consistent with cosmochemical evidence in our own Solar System.

Multi-wavelength radially resolved observations of grain properties, which were just barely becoming possible at the time of the last Protostars and Planets conference, are now providing a wealth of new constraints to the models. The overall radial segregation of dust aggregates of different sizes predicted by models is in general agreement with observations, however, the fast draining of solids towards the

inner disk predicted by models cannot reproduce the observations. A mechanism to slow down the radial drift is definitely required.

While the interpretation of the millimeter observations in terms of grain growth appears to be solid, the values of the dust opacities for the dust aggregates are still very uncertain. New computations or laboratory measurements for a range of grain composition and structure would represent a major step to put on very solid grounds the study of dust evolution in disks. Similarly, a major step in the understanding of the physical processes of grain growth in disks will be the extension of the grain-grain laboratory experiments to icy dust particles. These experiments are now been carried out and the initial results are expected in the coming years.

Armed with better constraints on the grain-grain collision outcomes, the global models of dust evolution in disks will also have to be advanced to the next stage. This will have to include a proper account of the gas and dust coevolution and the extension of the models to two and three dimensions, to account for vertical transport and azimuthal inhomogeneities, which are now routinely observed with ALMA.

On the observational side new and upgraded observing facilities at millimeter and centimeter wavelengths are offering an unprecedented opportunity to expand the detailed studies to faint objects and to resolve the detailed radial and vertical structure of the grain properties. In the coming years we expect that it will be possible to put strong constraints on the evolutionary timescale for the dust on the disk mid-plane and explore this process as a function of the central host star parameters and as a function of environment. The study of the dust and gas small scale structures in the disk, as well as their global distribution, will most likely allow us to solve the long standing problem of radial drift.

Acknowledgments. We thank M. Bizzarro, P. Caselli, C. Chandler, C. Dullemond, A. Dutrey, Th. Henning, A. Johansen, C. Ormel, R. Waters, and especially the referee, S. Okuzumi, for valuable comments and discussions on the content of this chapter. We thank F. Windmark for providing data for Fig. 2. The work reported here has been partly supported over the years by grants to INAF-Osservatorio Astrofisico di Arcetri from the MIUR, PRIN-INAF and ASI. Extended support from the Munich-IMPRS as well as ESO Studentship/Internship, DGDF and Scientific Visitor programmes in the period 2009-2013 is gratefully acknowledged. S. Andrews and T. Birnstiel acknowledge support from NASA Origins of Solar Systems grant NNX12AJ04G. A. Isella and J. M. Carpenter acknowledge support from NSF award AST-1109334. J. P. Williams acknowledges support from NSF award AST-1208911.

REFERENCES

Ábrahám P. et al. (2009) *Nature*, *459*, 224.
Adachi I. et al. (1976) *Progress of Theoretical Physics*, *56*, 1756.
Adams F. C. et al. (1990) *Astrophys. J.*, *357*, 606.
Andrews S. M. and Williams J. P. (2005) *Astrophys. J.*, *631*, 1134.
Andrews S. M. and Williams J. P. (2007) *Astrophys. J.*, *671*, 1800.
Andrews S. M. et al. (2012) *Astrophys. J.*, *744*, 162.
Andrews S. M. et al. (2013) *Astrophys. J.*, *771*, 129.
Ardila D. R. et al. (2007) *Astrophys. J.*, *665*, 512.
Armitage P. J. (2010) *Astrophysics of Planet Formation*, Cambridge University Press.
Ataiee S. et al. (2013) *A&A*, *553*, L3.
Bai X.-N. and Stone J. M. (2010) *ApJ*, *722*, 1437.
Banzatti A. et al. (2011) *Astron. Astrophys.*, *525*, A12.
Barge P. and Sommeria J. (1995) *Astron. Astrophys.*, *295*, L1.
Beckwith S. V. W. and Sargent A. I. (1991) *ApJ*, *381*, 250.
Beckwith S. V. W. et al. (2000) *PP IV*, p. 533.
Birnstiel T. et al. (2009) *Astron. Astrophys.*, *503*, L5.
Birnstiel T. et al. (2010a) *Astron. Astrophys.*, *513*, A79.
Birnstiel T. et al. (2010b) *Astron. Astrophys.*, *516*, L14.
Birnstiel T. et al. (2011) *Astron. Astrophys.*, *525*, A11.
Birnstiel T. et al. (2012) *Astron. Astrophys.*, *539*, A148.
Birnstiel T. et al. (2013) *Astron. Astrophys.*, *550*, L8.
Blum J. (2006) *Advances in Physics*, *55*, 881.
Blum J. and Wurm G. (2000) *Icarus*, *143*, 138.
Blum J. and Wurm G. (2008) *Annu. Rev. Astron. Astrophys.*, *46*, 21.
Blum J. et al. (2000) *Physical Review Letters*, *85*, 2426.
Bockelée-Morvan D. et al. (2002) *Astronomy and Astrophysics*, *384*, 1107.
Boehler Y. et al. (2013) *Mon. Not. R. Astron. Soc.*, *431*, 1573.
Bohren C. F. and Huffman D. R. (1983) *Absorption and scattering of light by small particles*, Wiley.
Bouwman J. et al. (2001) *Astron. Astrophys.*, *375*, 950.
Brauer F. et al. (2007) *A&A*, *469*, 1169.
Brauer F. et al. (2008a) *Astron. Astrophys.*, *480*, 859.
Brauer F. et al. (2008b) *Astron. Astrophys.*, *487*, L1.
Carballido A. et al. (2006) *MNRAS*, *373*, 1633.
Carballido A. et al. (2010) *Mon. Not. R. Astron. Soc.*, *405*, 2339.
Chatterjee S. and Tan J. C. (2014) *Astrophys. J.*, *780*, 53.
Chiang E. and Laughlin G. (2013) *MNRAS*, *431*, 3444.
Chiang E. I. and Goldreich P. (1997) *Astrophys. J.*, *490*, 368.
Chiang E. I. et al. (2001) *ApJ*, *547*, 1077.
Chiang H.-F. et al. (2012) *Astrophys. J.*, *756*, 168.
Chokshi A. et al. (1993) *Astrophys. J.*, *407*, 806.
Ciesla F. J. (2009) *Icarus*, *200*, 655.
Clampin M. et al. (2003) *Astron. J.*, *126*, 385.
Connelly J. N. et al. (2012) *Science*, *338*, 651.
Cossins P. et al. (2010) *Mon. Not. R. Astron. Soc.*, *407*, 181.
Cuzzi J. N. and Hogan R. C. (2003) *Icarus*, *164*, 127.
Cuzzi J. N. et al. (1993) *Icarus*, *106*, 102.
D'Alessio P. et al. (2001) *ApJ*, *553*, 321.
D'Alessio P. et al. (2006) *Astrophys. J.*, *638*, 314.
Dauphas N. and Chaussidon M. (2011) *Annual Review of Earth and Planetary Sciences*, *39*, 351.
de Gregorio-Monsalvo I. et al. (2013) *Astron. Astrophys.*, *557*, A133.
Dominik C. and Dullemond C. P. (2008) *Astron. Astrophys.*, *491*, 663.
Dominik C. and Nübold H. (2002) *Icarus*, *157*, 173.
Dominik C. and Tielens A. G. G. M. (1997) *Astrophys. J.*, *480*, 647.
Dominik C. et al. (2007) *PP V*, p. 783.
Douglas T. A. et al. (2013) *Mon. Not. R. Astron. Soc.*, *433*, 2064.

Draine B. T. (2006) *ApJ*, *636*, 1114.
Dubrulle B. et al. (1995) *Icarus*, *114*, 237.
Duchêne G. et al. (2010) *Astrophys. J.*, *712*, 112.
Dullemond C. P. and Dominik C. (2004) *Astron. Astrophys.*, *421*, 1075.
Dullemond C. P. and Dominik C. (2005) *Astron. Astrophys.*, *434*, 971.
Dullemond C. P. and Monnier J. D. (2010) *Annu. Rev. Astron. Astrophys.*, *48*, 205.
Dullemond C. P. et al. (2001) *Astrophys. J.*, *560*, 957.
Dullemond C. P. et al. (2007) *Protostars and Planets V*, pp. 555–572.
Eisner J. A. et al. (2008) *Astrophys. J.*, *683*, 304.
Evans II N. J. et al. (2009) *Astrophys. J. Suppl.*, *181*, 321.
Foster J. B. et al. (2013) *Mon. Not. R. Astron. Soc.*, *428*, 1606.
Fromang S. and Nelson R. P. (2005) *Monthly Notices of the Royal Astronomical Society: Letters*, *364*, L81.
Fromang S. and Nelson R. P. (2009) *Astron. Astrophys.*, *496*, 597.
Fromang S. et al. (2011) *Astron. Astrophys.*, *534*, A107.
Fukagawa M. et al. (2010) *PASJ*, *62*, 347.
Furlan E. et al. (2006) *Astrophys. J. Suppl.*, *165*, 568.
Garaud P. (2007) *Astrophys. J.*, *671*, 2091.
Garaud P. et al. (2013) *Astrophys. J.*, *764*, 146.
Goldreich P. and Ward W. R. (1973) *ApJ*, *183*, 1051.
Gräfe C. et al. (2013) *Astron. Astrophys.*, *553*, A69.
Greaves J. S. and Rice W. K. M. (2010) *Mon. Not. R. Astron. Soc.*, *407*, 1981.
Guilloteau S. et al. (2011) *Astron. Astrophys.*, *529*, A105.
Gundlach B. et al. (2011) *Icarus*, *214*, 717.
Güttler C. et al. (2010) *Astron. Astrophys.*, *513*, A56.
Hartmann L. (2009) *Accretion Processes in Star Formation: Second Edition*, Cambridge University Press.
Hayashi C. (1981) *Prog. Theor. Phys. Suppl.*, *70*, 35.
Heim L.-O. et al. (1999) *Physical Review Letters*, *83*, 3328.
Hirashita H. and Kuo T.-M. (2011) *MNRAS*, *416*, 1340.
Hsieh H.-F. and Gu P.-G. (2012) *ApJ*, *760*, 119.
Hubbard A. (2012) *MNRAS*, *426*, 784.
Hughes A. L. H. and Armitage P. J. (2012) *MNRAS*, *423*, 389.
Hughes A. M. et al. (2008) *Astrophys. J.*, *678*, 1119.
Isella A. et al. (2006) *Astron. Astrophys.*, *451*, 951.
Isella A. et al. (2007) *Astron. Astrophys.*, *469*, 213.
Isella A. et al. (2010) *Astrophys. J.*, *714*, 1746.
Isella A. et al. (2012) *Astrophys. J.*, *747*, 136.
Jacquet E. (2013) *Astronomy & Astrophysics*, *551*, 75.
Johansen A. and Klahr H. (2005) *ApJ*, *634*, 1353.
Johansen A. et al. (2009) *Astrophys. J.*, *697*, 1269.
Jørgensen J. K. et al. (2009) *Astron. Astrophys.*, *507*, 861.
Juhász A. et al. (2010) *Astrophys. J.*, *721*, 431.
Juhász A. et al. (2012) *Astrophys. J.*, *744*, 118.
Juvela M. et al. (2013) *Astron. Astrophys.*, *556*, A63.
Keller C. and Gail H.-P. (2004) *Astron. Astrophys.*, *415*, 1177.
Kelly B. C. et al. (2012) *Astrophys. J.*, *752*, 55.
Kempf S. et al. (1999) *Icarus*, *141*, 388.
Kessler-Silacci J. et al. (2006) *Astrophys. J.*, *639*, 275.
Kessler-Silacci J. E. et al. (2007) *Astrophys. J.*, *659*, 680.
Keto E. and Caselli P. (2008) *Astrophys. J.*, *683*, 238.
Klahr H. H. and Henning T. (1997) *Icarus*, *128*, 213.
Kley W. and Lin D. N. C. (1992) *ApJ*, *397*, 600.
Kornet K. et al. (2001) *A&A*, *378*, 180.
Kothe S. et al. (2010) *Astrophys. J.*, *725*, 1242.
Kothe S. et al. (2013) *Icarus*, *225*, 75.
Krause M. and Blum J. (2004) *Physical Review Letters*, *93*, 2, 021103.
Kretke K. A. and Lin D. N. C. (2007) *ApJ*, *664*, L55.
Kruegel E. and Siebenmorgen R. (1994) *Astron. Astrophys.*, *288*, 929.
Kudo T. et al. (2008) *Astrophys. J. Lett.*, *673*, L67.
Kwon W. et al. (2009) *Astrophys. J.*, *696*, 841.
Laibe G. et al. (2008) *Astron. Astrophys.*, *487*, 265.
Laibe G. et al. (2012) *A&A*, *537*, 61.
Lee M. H. (2000) *Icarus*, *143*, 74.
Liu Y. et al. (2012) *Astron. Astrophys.*, *546*, A7.
Lodders K. (2003) *ApJ*, *591*, 1220.
Lommen D. et al. (2009) *Astron. Astrophys.*, *495*, 869.
Luhman K. L. (2007) *Astrophys. J. Suppl.*, *173*, 104.
Luhman K. L. et al. (2010) *Astrophys. J. Suppl.*, *186*, 111.
Lynden-Bell D. and Pringle J. E. (1974) *MNRAS*, *168*, 603.
Mann R. K. and Williams J. P. (2010) *Astrophys. J.*, *725*, 430.
Markiewicz W. J. et al. (1991) *A&A*, *242*, 286.
Mathews G. S. et al. (2012) *Astrophys. J.*, *745*, 23.
Mathews G. S. et al. (2013) *Astron. Astrophys.*, *557*, A132.
Mathis J. S. et al. (1977) *ApJ*, *217*, 425.
Matthews L. S. et al. (2012) *Astrophys. J.*, *744*, 8.
McClure M. K. et al. (2013) *Astrophys. J.*, *775*, 114.
Meru F. et al. (2013) *Astrophys. J. Lett.*, *774*, L4.
Miyake K. and Nakagawa Y. (1993) *Icarus*, *106*, 20.
Mizuno H. et al. (1988) *A&A*, *195*, 183.
Morfill G. E. and Voelk H. J. (1984) *Astrophys. J.*, *287*, 371.
Mulders G. D. and Dominik C. (2012) *Astron. Astrophys.*, *539*, A9.
Mulders G. D. et al. (2013) *Astron. Astrophys.*, *549*, A112.
Nakagawa Y. et al. (1981) *Icarus*, *45*, 517.
Nakagawa Y. et al. (1986) *Icarus*, *67*, 375.
Natta A. and Testi L. (2004) in: *Star Formation in the Interstellar Medium: In Honor of David Hollenbach*, vol. 323 of *Astronomical Society of the Pacific Conference Series*, (edited by D. Johnstone, F. C. Adams, D. N. C. Lin, D. A. Neufeeld, and E. C. Ostriker), pp. 279–+.
Natta A. et al. (2007) *Protostars and Planets V*, pp. 767–781.
Ohtsuki K. et al. (1990) *Icarus*, *83*, 205.
Okuzumi S. (2009) *ApJ*, *698*, 1122.
Okuzumi S. et al. (2009) *ApJ*, *707*, 1247.
Okuzumi S. et al. (2011a) *ApJ*, *731*, 95.
Okuzumi S. et al. (2011b) *Astrophys. J.*, *731*, 96.
Okuzumi S. et al. (2012) *Astrophys. J.*, *752*, 106.
Oliveira I. et al. (2011) *Astrophys. J.*, *734*, 51.
Ormel C. W. and Cuzzi J. N. (2007) *Astron. Astrophys.*, *466*, 413.
Ormel C. W. and Okuzumi S. (2013) *ApJ*, *771*, 44.
Ormel C. W. et al. (2007) *Astron. Astrophys.*, *461*, 215.
Ormel C. W. et al. (2008) *Astrophys. J.*, *679*, 1588.
Ormel C. W. et al. (2009) *Astron. Astrophys.*, *502*, 845.
Ormel C. W. et al. (2011) *Astron. Astrophys.*, *532*, A43.
Ossenkopf V. (1993) *Astron. Astrophys.*, *280*, 617.
Ossenkopf V. and Henning T. (1994) *Astron. Astrophys.*, *291*, 943.
Pagani L. et al. (2010) *Science*, *329*, 1622.
Pan L. and Padoan P. (2010) *Journal of Fluid Mechanics*, *661*, 73.
Pan L. and Padoan P. (2013) *Astrophys. J.*, *776*, 12.
Panić O. et al. (2008) *Astron. Astrophys.*, *491*, 219.
Paradis D. et al. (2010) *Astron. Astrophys.*, *520*, L8.
Paszun D. and Dominik C. (2006) *Icarus*, *182*, 274.
Pérez L. M. et al. (2012) *Astrophys. J. Lett.*, *760*, L17.
Piétu V. et al. (2007) *Astron. Astrophys.*, *467*, 163.
Pinilla P. et al. (2012a) *Astron. Astrophys.*, *545*, A81.
Pinilla P. et al. (2012b) *Astron. Astrophys.*, *538*, A114.

Pinilla P. et al. (2013) *Astron. Astrophys.*, *554*, A95.
Pinte C. et al. (2007) *Astron. Astrophys.*, *469*, 963.
Pinte C. et al. (2008) *Astron. Astrophys.*, *489*, 633.
Pollack J. B. et al. (1994) *Astrophys. J.*, *421*, 615.
Poppe T. et al. (2000) *Astrophys. J.*, *533*, 472.
Qi C. et al. (2013) *Science*, *341*, 630.
Quanz S. P. et al. (2011) *Astrophys. J.*, *738*, 23.
Quanz S. P. et al. (2012) *Astron. Astrophys.*, *538*, A92.
Ricci L. et al. (2010a) *Astron. Astrophys.*, *521*, A66.
Ricci L. et al. (2010b) *Astron. Astrophys.*, *512*, A15.
Ricci L. et al. (2011) *Astron. Astrophys.*, *525*, A81.
Ricci L. et al. (2012a) *Astrophys. J. Lett.*, *761*, L20.
Ricci L. et al. (2012b) *Astron. Astrophys.*, *540*, A6.
Ricci L. et al. (2013) *Astrophys. J. Lett.*, *764*, L27.
Rodmann J. et al. (2006) *Astron. Astrophys.*, *446*, 211.
Ros K. and Johansen A. (2013) *A&A*, *552*, 137.
Rosenfeld K. A. et al. (2013) *Astrophys. J.*, *775*, 136.
Roy A. et al. (2013) *Astrophys. J.*, *763*, 55.
Rozyczka M. et al. (1994) *Astrophysical Journal v.423*, *423*, 736.
Sadavoy S. I. et al. (2013) *Astrophys. J.*, *767*, 126.
Safronov V. S. (1969) *Evolution of the protoplanetary cloud and formation of the earth and planets. English translation (1972).*
Salter D. M. et al. (2010) *Astron. Astrophys.*, *521*, A32.
Schmitt W. et al. (1997) *Astron. Astrophys.*, *325*, 569.
Schräpler R. and Blum J. (2011) *Astrophys. J.*, *734*, 108.
Schräpler R. and Henning T. (2004) *ApJ*, *614*, 960.
Scott E. R. D. and Krot A. N. (2005) *Astrophys. J.*, *623*, 571.
Shakura N. I. and Sunyaev R. A. (1973) *A&A*, *24*, 337.
Shetty R. et al. (2009) *Astrophys. J.*, *696*, 2234.
Shu F. et al. (1994) *ApJ*, *429*, 781.
Shu F. H. et al. (2001) *ApJ*, *548*, 1029.
Sicilia-Aguilar A. et al. (2007) *ApJ*, *659*, 1637.
Sirono S.-I. (2011a) *ApJL*, *733*, L41.
Sirono S.-I. (2011b) *ApJ*, *735*, 131.
Smoluchowski M. V. (1916) *Physik. Zeit.*, *17*, 557.
Steinacker J. et al. (2010) *Astron. Astrophys.*, *511*, A9.
Stepinski T. F. and Valageas P. (1996) *Astron. Astrophys.*, *309*, 301.
Stepinski T. F. and Valageas P. (1997) *Astron. Astrophys.*, *319*, 1007.
Stepnik B. et al. (2003) *Astron. Astrophys.*, *398*, 551.
Sterzik M. F. and Morfill G. E. (1994) *Icarus*, *111*, 536.
Suttner G. and Yorke H. W. (2001) *Astrophys. J.*, *551*, 461.
Suttner G. et al. (1999) *Astrophys. J.*, *524*, 857.
Suutarinen A. et al. (2013) *Astron. Astrophys.*, *555*, A140.
Suyama T. et al. (2012) *ApJ*, *753*, 115.
Takeuchi T. and Lin D. N. C. (2002) *ApJ*, *581*, 1344.
Tanaka H. et al. (2005) *Astrophys. J.*, *625*, 414.
Teiser J. and Wurm G. (2009a) *Astron. Astrophys.*, *505*, 351.
Teiser J. and Wurm G. (2009b) *Mon. Not. R. Astron. Soc.*, *393*, 1584.
Teiser J. et al. (2011) *Icarus*, *215*, 596.
Testi L. et al. (2001) *ApJ*, *554*, 1087.
Testi L. et al. (2003) *A&A*, *403*, 323.
Tobin J. J. et al. (2013) *Astrophys. J.*, *771*, 48.
Trotta F. et al. (2013) *Astron. Astrophys.*, *558*, A64.
Ubach C. et al. (2012) *Mon. Not. R. Astron. Soc.*, *425*, 3137.
Uribe A. L. et al. (2011) *Astrophys. J.*, *736*, 85.
Urpin V. A. (1984) *Soviet Ast.*, *28*, 50.
van Boekel R. et al. (2004) *Nature*, *432*, 479.
van Boekel R. et al. (2005) *Astron. Astrophys.*, *437*, 189.
van der Marel N. et al. (2013) *Science*, *340*, 1199.
Veneziani M. et al. (2010) *Astrophys. J.*, *713*, 959.
Voelk H. J. et al. (1980) *Astron. Astrophys.*, *85*, 316.
Wada K. et al. (2008) *Astrophys. J.*, *677*, 1296.
Wada K. et al. (2009) *Astrophys. J.*, *702*, 1490.
Weidenschilling S. J. (1977) *Mon. Not. R. Astron. Soc.*, *180*, 57.
Weidenschilling S. J. (1977) *Ap&SS*, *51*, 153.
Weidenschilling S. J. (1980) *Icarus*, *44*, 172.
Weidenschilling S. J. (1984) *Icarus*, *60*, 553.
Weidenschilling S. J. (1997) *Icarus*, *127*, 290.
Weidenschilling S. J. and Cuzzi J. N. (1993) in: *Protostars and Planets III*, (edited by E. H. Levy and J. I. Lunine), pp. 1031–1060.
Weidenschilling S. J. and Ruzmaikina T. V. (1994) *Astrophys. J.*, *430*, 713.
Weintraub D. A. et al. (1989) *Astrophys. J. Lett.*, *340*, L69.
Whipple F. L. (1972) in: *From Plasma to Planet*, (edited by A. Elvius), p. 211.
Whipple F. L. (1972) *From Plasma to Planet*, p. 211.
Williams J. P. and Cieza L. A. (2011) *Annu. Rev. Astron. Astrophys.*, *49*, 67.
Williams J. P. et al. (2005) *Astrophys. J.*, *634*, 495.
Williams J. P. et al. (2013) *Mon. Not. R. Astron. Soc.*, *435*, 1671.
Wilner D. J. et al. (2005) *ApJL*, *626*, L109.
Windmark F. et al. (2012a) *Astron. Astrophys.*, *544*, L16.
Windmark F. et al. (2012b) *Astron. Astrophys.*, *540*, A73.
Wisniewski J. P. et al. (2008) *Astrophys. J.*, *682*, 548.
Wolf S. et al. (2003) *Astrophys. J.*, *588*, 373.
Wolf S. et al. (2008) *Astrophys. J. Lett.*, *674*, L101.
Wolf S. et al. (2012) *Astron. Astrophys. Rev.*, *20*, 52.
Woody D. P. et al. (1989) *Astrophys. J. Lett.*, *337*, L41.
Wurm G. et al. (2005) *Icarus*, *178*, 253.
Youdin A. N. and Goodman J. (2005) *ApJ*, *620*, 459.
Youdin A. N. and Lithwick Y. (2007) *Icarus*, *192*, 588.
Youdin A. N. and Shu F. H. (2002) *Astrophys. J.*, *580*, 494.
Zhukovska S. et al. (2008) *A&A*, *479*, 453.
Zsom A. et al. (2010) *Astron. Astrophys.*, *513*, A57.
Zsom A. et al. (2011) *Astron. Astrophys.*, *534*, 73.

This 2-column preprint was prepared with the AAS LaTeX macros v5.2.